

October 2013

Uncovering the Molecular Link Between miR156.SPL15 and Carotenoid Accumulation in Arabidopsis

Davood Emami Meybodi
The University of Western Ontario

Supervisor
Dr. Abdelali Hannoufa, Dr. Percival-Smith
The University of Western Ontario

Graduate Program in Biology

A thesis submitted in partial fulfillment of the requirements for the degree in Master of Science

© Davood Emami Meybodi 2013

Follow this and additional works at: <http://ir.lib.uwo.ca/etd>

 Part of the [Agriculture Commons](#), [Biology Commons](#), [Biotechnology Commons](#), [Food Biotechnology Commons](#), and the [Molecular Biology Commons](#)

Recommended Citation

Emami Meybodi, Davood, "Uncovering the Molecular Link Between miR156.SPL15 and Carotenoid Accumulation in Arabidopsis" (2013). *Electronic Thesis and Dissertation Repository*. Paper 1672.

UNCOVERING THE MOLECULAR LINK BETWEEN *miR156/SPL15* AND
CAROTENOID ACCUMULATION IN ARABIDOPSIS

(Thesis format: Monograph)

by

Davood Emami Meybodi

Graduate Program in Biology

A thesis submitted in partial fulfillment
of the requirements for the degree of
Master of Science

The School of Graduate and Postdoctoral Studies
The University of Western Ontario
London, Ontario, Canada

© Davood Emami Meybodi 2014

Abstract

Carotenoid Cleavage Dioxygenases (*CCDs*) are an enzyme family that cleaves specific double bonds in carotenoids. *MicroR156* in *Arabidopsis* regulates a network of genes by repressing 10 *SPL* genes, among which, *SPL15* was found to regulate shoot branching and carotenoid accumulation. The expression of *CCD1*, *CCD4*, *CCD7*, *CCD8*, *NCED2*, *NCED3*, *NCED5*, *NCED6*, *NCED9* and *SPL15* was evaluated in siliques at 10 days post anthesis and in 10-day-old roots in *Arabidopsis* wild type, *sk156* (*miR156* overexpression mutant), *RS105* (*miR156* overexpression line), *spl15* (*SPL15* knockout mutant) and two 35S:*SPL15* lines. Results showed that most of *CCD/NCED* genes were affected both in the roots and siliques by function of *miR156*. In addition transcript levels of four *CCD/NCED* genes were up regulated in 35S:*SPL15* lines. To test binding of *SPL15* to affected *CCD/NCED* genes, 35S:*SPL15*-GFP transgenic lines were generated and three independent lines were subjected to ChIP-qPCR. The results revealed strong and selective occupancy of *SPL15* on the promoter regions of candidate *CCD/NCED* genes. In addition, *sk156* and *RS105* had larger size of elaioplasts and plastoglobules compared to wild type. My results indicate that *miR156/SPL15* control carotenoid accumulation by regulating expression of *CCD/NCED* genes and by increasing the cell's capacity to store carotenoids.

Keywords

Arabidopsis, carotenoids, gene regulation, *CCD/NCED*, *SPL15*, *miR156*

Dedication

This thesis is dedicated to my parents for all of their support and endless love

Acknowledgments

I would like to thank my supervisor, Dr. Abdelali Hannoufa, for giving me the opportunity to work in this project. Thanks for your support before I came here, so that I could start my studies on time. I am grateful to my co-supervisor, Dr. Anthony Percival Smith, for his guidance and being supportive during last two years. I would like to thank my advisory committee members Dr. Sangeeta Dhaubhadel for her critical editing of my thesis and guidance during my research and Dr. Denis Maxwell for his advice and helpful suggestions.

I am grateful to Dr. Richard Gardiner for the friendly manner and for teaching me transmission electron microscopy. I would like thank to Prof. Norm Huner for giving me his time for scientific discussions.

I am very thankful to my lab mates and friends who always helped me with experiments and for providing a friendly environment: Ying Wang, Shailu Lakshminarayan, Arun Kumaran, Banyae Aung, Reza Saberianfar, Nadia Morales, and Lisa Amyot.

I would like to express my gratitude to the staff of the University of Western Ontario and Agriculture and Agri-Food Canada, especially Carol Curtis, Arzie Chant, Dorothy Drew, Winona Gadapati and Shelly Snook for all their help.

I would like to thank my family, for all of their support and motivations over the years. Lastly, I would like to have a special thank you to my wife for all of her support and love during my Master study.

Table of Contents

Abstract	ii
Dedication	iii
Acknowledgments	iv
Table of Contents	v
List of Tables	viii
List of Figures	ix
List of Appendices	xi
List of Abbreviations	xii
1. INTRODUCTION AND BACKGROUND	1
1.1 Carotenoid Biosynthesis Pathway	2
1.2 Regulation of Carotenoid Biosynthesis	4
1.2.1 Developmental and environmental regulation	4
1.2.2 Transcriptional and epigenetic regulation.....	5
1.3 Carotenoid Catabolism	6
1.3.1 Carotenoid cleavage dioxygenases	6
1.4 Carotenoid Sequestration and Storage	9
1.5 Small RNA and miRNA	11
1.6 Role of <i>microRNA156</i> in Carotenoid Regulation	12
1.7 Proposed Research	14
2 MATERIAL AND METHODS	17
2.1 Plant Materials and Growth Conditions	17
2.2 RNA Extraction from Arabidopsis Tissue	18
2.3 DNA Extraction from Arabidopsis Tissues	18

2.4	Preparation of Chemically Competent <i>E. coli</i> Cells	19
2.5	Preparation of Electro-Competent <i>Agrobacterium tumefaciens</i> Cells.....	19
2.6	Plasmid Extraction.....	20
2.7	DNA Sequencing	21
2.8	Primer Design	21
2.9	Generating SPL15-GFP Fusion Constructs	22
2.10	Arabidopsis Transformation.....	23
2.11	Screening for Arabidopsis Transformants	23
2.12	Chromatin Immuno-Precipitation (ChIP)-qPCR	24
2.13	Transmission Electron Microscopy	28
2.14	Agarose Gel Electrophoresis	29
2.15	Real Time-qPCR Analysis.....	29
3	RESULTS	32
3.1	Assessing the Specificity of DNA Fragments Amplified by PCR	32
3.2	Analysis of <i>CCD/NCED</i> Expression in <i>miR156</i> Overexpression Plants.....	32
3.2.1	Effect of <i>miR156</i> on <i>CCD/NCED</i> transcript levels in roots	32
3.2.2	Effect of <i>miR156</i> on <i>CCD/NCED</i> transcript levels in siliques	33
3.3	Analysis of the Effect of SPL15 on the Expression of <i>CCD/NCED</i> Genes.....	38
3.3.1	Effect of SPL15 on transcript levels of <i>CCD/NCED</i> genes in roots and siliques	38
3.3.2	The effect of SPL15 on expression of <i>CCD/NCED</i> genes in siliques	39
3.3.3	The link between number of GTAC element and <i>CCD/NCED</i> transcript levels	40
3.4	Analysis of SPL15 Binding to Promoters of <i>CCD/NCED</i> Genes	49
3.5	Effect of MiR156 on the Anatomical Structure of Seed Elaioplasts.....	58
4	DISCUSSION	61

4.1	Overview	61
4.2	MiR156 Has a General Suppressive Effect on <i>CCD/NCED</i> Expression in Roots	62
4.3	<i>MiR156</i> Exhibits Differential Effects on Expression of <i>CCD/NCED</i> Genes ...	64
4.4	The Effect of <i>SPL15</i> on the Transcript Level of <i>CCD/NCED</i> Genes.....	65
4.5	<i>SPL15</i> Binding to Promoters of <i>CCD/NCED</i> Genes	66
4.6	Overexpression of miR156 Affects the Anatomical Structure of Plastids in Seeds	67
4.7	Conclusions and Prospective for Future Research	69
	References	72
	Appendix 1.....	82
	Curriculum Vitae	84

List of Tables

Table 1: The Buffers used in the ChIP assay	27
Table 2: List of primers that were used in this study	30

List of Figures

Figure 1. Carotenoid biosynthesis pathway	3
Figure 2. Transcript levels of <i>CCD</i> and <i>NCED</i> genes in the roots of 10 day-old seedlings of WT, <i>sk156</i> and <i>RS105 Arabidopsis</i> plants.	35
Figure 3. Transcript levels of <i>CCD</i> and <i>NCED</i> genes in 10 DPA (day post anthesis) siliques of WT, <i>sk156</i> and <i>RS105 Arabidopsis</i> plants.....	37
Figure 4. Transcript levels of <i>SPL15</i> in roots of 10 day-old seedlings (A) and 10 DPA (day post anthesis) siliques (B) of WT, <i>sk156</i> and <i>RS105</i> , <i>spl15</i> and 35S: <i>SPL15 Arabidopsis</i> plants.	42
Figure 5. Transcript levels of <i>CCD</i> and <i>NCED</i> genes in roots of 10 day-old seedlings of WT, <i>spl15</i> and 35S: <i>SPL15 Arabidopsis</i> plants.	44
Figure 6. Transcript levels of <i>CCD</i> and <i>NCED</i> genes in 10 DPA siliques of WT, <i>spl15</i> and 35S: <i>SPL15 Arabidopsis</i> plants.	46
Figure 7. Schematic representation of the positions of GTAC elements in the promoter regions of <i>CCD</i> and <i>NCED</i> genes.....	48
Figure 8. Map of the <i>SPL15</i> -GFP fusion construct.	51
Figure 9. PCR amplification of the <i>SPL15</i> +GFP fragment in different transgenic 35S: <i>SPL15</i> -GFP <i>Arabidopsis</i> lines (A); RT-qPCR analysis of <i>SPL15</i> transcript in the same transgenic lines (B).	53
Figure 10. qPCR analysis of DNA generated from CHIP analysis of 35S: <i>SPL15</i> -GFP lines using anti-GFP antibody.....	55
Figure 11. Consensus sequences in the vicinity of core GTAC elements in <i>CCD/NCED</i> promoters showing strong binding (A) and no or weak binding (B) to <i>SPL15</i>	57
Figure 12. Transmission electron micrographs of <i>Arabidopsis</i> seed elaioplasts.	59

Figure 13. The averages size of 35 elaioplasts in mature seeds of *sk156*, *RS105* and wild type.. 60

Figure 14. A proposed model for the regulatory role of miR156 in carotenoid accumulation....70

List of Appendices

Appendix 1. The BLAST search results of <i>CCD</i> , <i>NCED</i> and <i>SPL15</i> PCR products to determine their specificity.....	82
--	----

List of Abbreviations

ABA	Absciscic Acid
BLAST	Basic Local Alignment Search Tool
Bp	base pair(s)
C	Centigrade
CaMV	Cauliflower mosaic virus
Cat #	Catalog Number
cDNA	Complimentary DNA
CDS	Coding DNA sequences
ChIP	Chromatin Immuno Precipitation
ddH ₂ O	Double-distilled Water
DNA	Deoxyribonucleic acid
dNTP	Deoxyribonucleic triphosphates
<i>E. coli</i>	<i>Escherichia coli</i>
EDTA	Ethylenediaminetetraacetic acid
EtOH	Ethanol
G	G Force
GFP	Green Fluorescent Protein
h	Hour(s)
L	Liter(s)
LB	Luria Broth
M	Molar
mg	Milligram(s)
min	Minute(s)
miRNAs	Micro-RNAs

ml	Milliliter(s)
mM	Millimolar(s)
MS	Murashige and Skoog medium
NaCl	Sodium Chloride
nat-siRNAs	Natural Antisense Transcripts
OD 600	Optical density at 600 nm
PCR	Polymerase Chain Reaction
PMSF	phenylmethanesulfonylfluoride
qPCR	Quantitative PCR
qRT-PCR	Reverse Transcription qPCR
RNA	Ribonucleic acid
RT	Room Temperature
SDS	Sodium Dodecyl Sulphate
siRNAs	Small Interfering RNAs
smRNAs	Small RNAs
TBE	Tris/Borate/EDTA Buffer
Tris	Tris-(hydroxymethyl)-methylamine
U	Unit
UV	Ultra-violet
v/v	Volume/volume
Vol	Volume
w/v	Weight/volume
μl	Microliter(s)
μg	Microgram(s)

1. INTRODUCTION AND BACKGROUND

Carotenoids are abundant isoprenoid pigments with more than 700 members (Britton et al., 2004). Isoprenoids are precursors to a range of secondary metabolites, such as abscisic acid (ABA), gibberellin, chlorophyll and carotenoids (Cazzonelli, 2011). Carotenoids are synthesized in all photosynthetic organisms such as plants and algae (Wurtzel et al., 2012) as well as some non-photosynthetic organisms such as fungi, bacteria and aphids (Iniesta et al., 2008; Li et al., 2008; Moran and Jarvik, 2010). They contribute to the different colors of fruits and flowers, and are essential for attracting pollinators such as birds and insects, to flowers (Howitt and Pogson, 2006). Carotenoids play critical roles in the physiological functions of photosynthetic organisms, including photosystem assembly, increased light harvesting, protection from photo-oxidative damage and free radical detoxification (Sandmann et al., 2006; Havaux et al., 2007; Li et al., 2008). Carotenoids can absorb a broader range of light than chlorophyll and transfer energy to it (Polivka and Frank, 2010), and thus carotenoids are essential for light harvesting; as up to 50 carotenoids can capture solar energy (Polivka and Frank, 2010). One of the most important functions of carotenoids is to strike a balance between light harvesting for photosynthetic processes while preventing photo oxidative damage caused by high levels of light (Cazzonelli, 2011). Some carotenoids, including beta-carotene, alpha carotene, gamma carotene and beta-cryptoxanthin are an important source of retinoid and vitamin A. These and other carotenoids, such as lycopene, can also act as antioxidants, which are essential for human diet and health (Fraser et al., 2007). In addition, carotenoids are economically important due to their use as colorants in the cosmetics and food industries, and as supplements in livestock and fish feed formulations (Umeno et al., 2005).

1.1 Carotenoid Biosynthesis Pathway

A simplified carotenoid biosynthesis pathway showing the main carotenoids that accumulate in *Arabidopsis* is presented in Figure 1. Carotenoid biosynthesis originates in the plastidal 2-C-methyl-D-erythriol 4-phosphate (MEP) pathway. The condensation of glyceraldehyde-3-phosphate and pyruvate generate 1-deoxy-D-xylulose-5-phosphate (DXP), a reaction catalyzed by 1-deoxy-D-xylulose-5-phosphate synthase (DXS), leads to dimethylallyl diphosphates (DMAPP) and isopentenyl diphosphate (IPP). Geranylgeranyl diphosphate (GGPP) is synthesized from the addition of IPP to DMAPP, GGPP is a precursor of several plastidial isoprenoids, including carotenoids (Bouvier et al., 2005). The condensation of two molecules of GGPP, which is catalyzed by phytoene synthase (PSY), is the first committed step in carotenoid biosynthesis, and gives rise to phytoene; a colorless carotenoid. There are four enzymes that are required for converting phytoene to lycopene (red carotenoid) in plants. These are phytoene desaturase (PDS), ζ -carotene desaturase (ZDS), carotenoid isomerase (CRTISO) and 15-cis- ζ -carotene isomerase (Z-ISO). Lycopene is found in many plant organs, such as tomato and watermelon fruits. Lycopene undergoes either α , β cyclizations to form α -carotene or β , β cyclizations to form β -carotene (Cazzonelli and Pogson, 2010). The hydroxylation of α -carotene and β -carotene produces xanthophylls, which include zeaxanthin, neoxanthin, violaxanthin and lutein. Conversion of violaxanthin to neoxanthin is the last step of the carotenoid biosynthesis pathway. Two apocarotenoid hormones, ABA and strigolactones are synthesized through the carotenoid pathway. ABA is synthesized through the cleavage of violaxanthin and neoxanthin to form xanthoxin (Frey et al., 2012), which is then converted to ABA (Ruiz-Sola and Rodriguez-Concepcion, 2012). Strigolactones are shoot branching inhibitors, and are synthesized from β -carotene through the action of carotenoid cleavage dioxygenases 7 and 8 (CCD7 and CCD8).

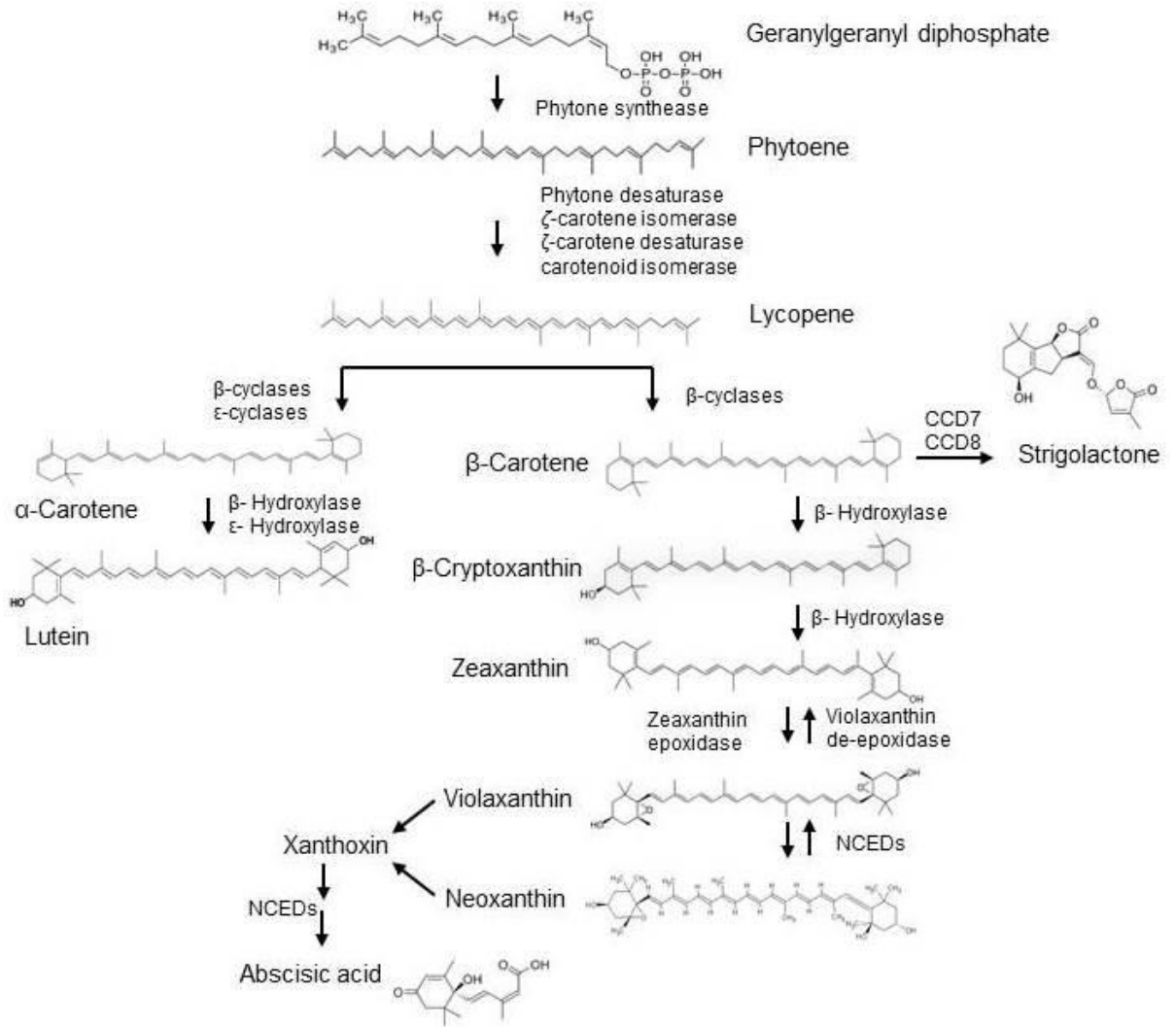


Figure 1. Carotenoid biosynthesis pathway

CCD (Carotenoid Cleavage Dioxygenases), *NCED* (9-cis epoxycarotenoid dioxygenase)

1.2 Regulation of Carotenoid Biosynthesis

1.2.1 Developmental and environmental regulation

Carotenoids accumulate in most plant tissues, including green and non-green ones. Carotenoid levels in green tissue are relatively conserved in many plant species, however, the content of carotenoids in non-green tissues such as seeds, fruits and flowers are dependent on various factors, such as types of plastids in different tissues and the physiological age of the plant (Howitt and Pogson, 2006). Carotenoid production can be regulated by both environmental and developmental factors (Cazzonelli and Pogson, 2010). For instance, carotenoid biosynthesis in tomato is regulated by a developmental signal, temperature and light stress (Ruiz-Sola and Rodriguez-Concepcion, 2012). During tomato fruit ripening, an increase in the production of DXS and PSY enzymes leads to the accumulation of carotenoids, especially lycopene (Giovannoni, 2001). In addition, during this stage chlorophylls are degraded and high amounts of carotenoids can be stored instead, causing the green color to change to red.

Carotenoid production is also highly associated with light to protect the photosynthetic apparatus from photo oxidative damage. In *Arabidopsis* most of the carotenoid biosynthesis enzymes such as DXS and PSY are up-regulated during light condition (Meier et al., 2011). In the dark when photosynthesis is not saturated, zeaxanthin is converted to violaxanthin by zeaxanthin epoxidase. However, in strong light when photosynthesis is saturated, violaxanthin is converted to zeaxanthin by the function of violaxanthin de-epoxidase enzyme. The inter conversion of these two carotenoids is the key step in plant adaptation to different light conditions.

1.2.2 Transcriptional and epigenetic regulation

Transcription factors (TFs) are sequence-specific DNA binding proteins that regulate and control transcription. A number of studies have shown the role of transcription factors in the regulation of carotenoid biosynthesis. For example, phytohormone-interaction factor (PIFs) are members of the helix-loop-helix transcription factor family, which can repress carotenoid regulation by binding to the promoter of *PSY* in the dark; however, by exposure of seedling to the light the PIFs are degraded, and thus, allow *PSY* to be expressed, and consequently enhance carotenoid biosynthesis (Toledo-Ortiz et al., 2010). The AtRAP2.2 transcription factor in Arabidopsis binds to the ATCTA motif in the promoter regions of *PSY* and *PDS* genes and enhances the transcript levels of both genes (Welsch et al., 2007). Also the *rap2.2* mutant line showed a decrease in transcript levels of both *PSY* and *PDS* which were accompanied by reduced levels of carotenoids (Welsch et al., 2007). In Arabidopsis, the transcript levels of some genes are related to carotenoid biosynthesis (Winter et al., 2007). For example, the balance between expression of *PSY* and *LCYB* genes is correlated to the amount of β -carotene in various plastids (Ruiz-Sola and Rodriguez-Concepcion, 2012).

Epigenetic mechanisms were also recently shown to play a role in regulating the carotenoid biosynthesis by affecting expression of carotenoid isomerase (*CRTISO*), which catalyzes a branch point in the carotenoid biosynthesis pathway (Cazzonelli et al., 2009). The *CCR1* gene encodes SET DOMAIN GROUP 8 (SDG8), which is required for expression of *CRTISO* genes. In *ccr1* mutants the level of *CRTISO* transcript is decreased due to reduced level of histone3 lysine4 tri-methylation (Cazzonelli et al., 2009).

1.3 Carotenoid Catabolism

1.3.1 Carotenoid cleavage dioxygenases

In photosynthetic tissues, the ratio between chlorophyll and carotenoid is an essential factor. In addition to the storage capacity of plastids, the level of carotenoids is dependent on the balance between catabolism and biosynthesis of carotenoids (Beisel et al., 2010; Ruiz-Sola and Rodriguez-Concepcion, 2012). Carotenoid catabolism is due mainly to enzymatic oxidation (Ruiz-Sola and Rodriguez-Concepcion, 2012). There are two types of enzymes that are involved in enzymatic oxidation of carotenoids; enzymes non-specific to carotenoids, such as peroxidases, and carotenoid-specific enzymes, such as carotenoid cleavage dioxygenases (*CCD*). These are a gene family that have been identified in many plant species, including avocado (Chernys and Zeevaart, 2000), petunia (Simkin et al., 2004), tomato (Burbidge et al., 1999), and Arabidopsis (Tan et al., 2003). In addition to plants, *CCD* genes have been found in bacteria, mouse, drosophila and humans (Redmond et al., 2001; Lindqvist and Andersson, 2002). In plants, *CCD* enzymes cleave specific double bonds in carotenoid molecules. Viviparous14 was the first protein identified in Maize (*Zea mays*), which showed cleavage of 11, 12 double bonds to produce xanthoxin.

The Arabidopsis genome encodes nine members of *CCD* genes, which are divided into two sub-groups (Tan et al., 2003). Four of these, the carotenoid cleavage dioxygenases (*CCD1*, *CCD4*, *CCD7* and *CCD8*) are closely related to each other. The remaining five, 9-sis epoxy-carotenoid dioxygenase (*NCED2*, *NCED3*, *NCED5*, *NCED6* and *NCED9*) are closely related to each other but not to *CCD* genes (Ohmiya, 2009). Different types of *CCD* genes are distinguished by their specific cleavage site and/or carotenoid substrate (Cardon et al., 1997). One or more *CCD/NCED* could cleave carotenoids to produce apocarotenoids with various structures and functions (Walter et al., 2010). Apocarotenoids are important not only

for their vital physiological functions, but also for their role as precursors of hormones, and aroma, or as insect attraction compounds (Bouvier et al., 2005; Walter et al., 2010).

Among CCD enzymes, CCD1 is unique in its subcellular localization and activity (Ohmiya, 2009; Walter et al., 2010). Unlike other CCD and NCED enzymes, which reside in the plastid, CCD1 localizes in the cytoplasm (Strack et al., 2010). The Arabidopsis CCD1 (AtCCD1) symmetrically cleaves sites at 9, 10 (9', 10') in carotenoid backbones to produce various derivatives (Schmidt et al., 2006; Garcia-Limones et al., 2008). In addition, *AtCCD1* can cleave 5, 6 (5', 6') and 7, 8 (7', 8') double bonds (Huang et al., 2009; Ilg et al., 2009). Volatile compounds, such as β -ionone and β -cyclocitral, are derived from carotenoids by the action of CCD1 in flowers and fruits (Ohmiya, 2009). *CCD1* loss of function led to reduced levels of β -ionone in petunia (Ohmiya, 2009), and its overexpression resulted in enhanced β -ionone emissions and improved insect resistance in Arabidopsis (Wei et al., 2011)

The function of CCD4 is related to color, aroma and flavor of fruits and flowers in some plant species (Ohmiya, 2009). CCD4 is involved in the biosynthesis of some apocarotenoids such as corcin and safranal, which are commercially valuable (Bouvier et al., 2005). Bixin, which is widely used in the food and cosmetics industries, is synthesized by the cleavage of double bonds of lycopene by the action of CCD4 and its loss of function resulted in yellow petals in *Chrysanthemum morifolium* (Ohmiya et al., 2006). Some studies have shown that CCD4 cleaves at 9, 10 (9', 10') double bonds (Huang et al., 2009b; Rubio et al., 2008), However 7, 8 (7', 8') and 5, 6 (5', 6') cleavage activities of CCD4 have also been reported. *CCD7* and *CCD8* are mainly expressed in roots and are involved in β -carotene catabolism (Booker et al., 2004; Auldridge et al., 2006). One of the products generated by the actions of *CCD7* and *CCD8* is strigolactones (Gomez-Roldan et al., 2008) (Fig 1). The apocarotenoids

nature of strigolactones was confirmed by several experiments on carotenoid pathways in tomato, maize and sorghum (Matusova et al., 2005; Lopez-Raez et al., 2008). More recently, strigolactones were found in plant root exudates as a seed germination stimulant for root parasitic weeds (Xie et al., 2008; Xie and Yoneyama, 2010) and as a specific signal for producing fungi branching hyphal (Akiyama et al., 2005). In addition, strigolactones are shoot branching inhibitory phytohormones (Booker et al, 2004; Schwartz et al, 2004; Auldridge et al, 2006). Some genes, such as more axillary growth (*MAX*) 3 in Arabidopsis and ramosus (*RMS*) 5 in pea are orthologous to *CCD7* and *MAX4* in Arabidopsis and *RMS1* in pea are orthologous to *CCD8*. (Sorefan et al., 2003; Booker et al., 2004; Snowden et al., 2005; Arite et al., 2007). The mutants of these genes, *max3*, *max4*, *rms*, showed enhanced shoot branching (Turnbull et al, 2002; Johnson et al, 2006; Arite et al, 2007; Simons et al, 2007).

1.3.2 9-*cis* epoxy-carotenoid dioxygenase (NCED)

All five members of NCED proteins are involved in ABA biosynthesis, and are all located to plastids (Tan et al., 2003). ABA has various functions in seed dormancy, root growth, response to water deficiency and stomatal aperture (Nambara and Marion-Poll, 2005). ABA is synthesized in high amounts in vegetative tissues and then transported to seeds (Kanno et al., 2010). ABA accumulates at high levels during the maturation stage in developing seeds (Frey et al., 2004). Among NCED proteins, NCED5 is mostly bound to the thylakoid membrane, whereas NCED9 is found in the stroma. Other NCEDs (2, 3 and 6) are active in both the thylakoid and stroma (Tan et al., 2003). *NCED6* and *NCED9* expression is necessary for ABA biosynthesis in the endosperm and embryo, which further regulates seed dormancy

(Lefebvre et al., 2006). Expression of *NCED9* in embryo inhibits cell elongation through the production of ABA (Frey et al., 2012). The role of *NCED3* is related to response to water stress, whereas the rest of the *NCED* genes showed minor effects on water deficiency (Tan et al., 2003; Frey et al., 2012). A role for *NCED5* in seed dormancy was deduced from its increased expression at the maturation stage (Lefebvre et al., 2006). ABA derived from the activities of *NCED2* and *NCED3* was found to have little effect on seed dormancy (Kanno et al., 2010).

1.4 Carotenoid Sequestration and Storage

Although the rate of carotenoid biosynthesis is a critical factor in determining its steady-state level, the size and capacity of plastids to store carotenoids has a direct bearing on its accumulation (Cazzonelli and Pogson, 2010). Although all carotenoid biosynthesis genes are encoded by the nuclear genome, nearly all of carotenoid pigments and their enzymes are located in the plastid (Cazzonelli et al., 2009). Plastids are compartments within every plant cell except pollen (Neuhaus and Emes, 2000), in which carotenoids are sequestered and stored. The *high pigment (hp)-2* tomato mutant showed high level of fruit pigmentation and larger plastids (Kolotilin et al., 2007). Similarly, the *hp-3* mutant of tomato which has a lesion in zeaxanthin epoxidase and deficiency in ABA, has a larger plastid compartment and 30% more storage capacity compared to wild type (Galpaz et al., 2008). Carotenoids are stored in the plastoglobules and sequestered as a chlorophyll-carotenoid-protein complex in the thylakoid membranes of plastids (Austin et al., 2006). The plastoglobules are droplets of lipid or lipoprotein particles located in the plastid (Lichtenthaler and Peveling, 1966; Brehelin and Kessler, 2008). Some studies have shown plastoglobules form as blebs in the

stroma specifically on the thylakoid membrane or in the inner parts of the plastid envelope membrane (Ghosh et al., 1994; Kessler et al., 1999). There is a correlation between the number of plastoglobules and physiological and environmental events in plants (Austin et al., 2006). For instance, the etioplasts have more plastoglobules while they do not have fully developed thylakoids; however during plastid development or thylakoid biogenesis the number of plastoglobules is reduced (Lichtenthaler and Peveling, 1966). Plastoglobules contain various lipidic compounds such as free fatty acids, triacylglycerols, chlorophyll and carotenoids (Lichtenthaler and Peveling, 1966; Kaup et al., 2002).

Different types of plastids exist in plant cells, including chloroplasts (green plastid), leucoplasts (non-pigmented plastids), amyloplasts (starch-storing plastids), elaioplasts (lipid-storing plastids), chromoplasts (pigmented plastids), and etioplasts (dark-grown precursors of the chloroplast). The proplastid is the progenitor of all plastids and exists in embryogenic and meristematic cells (Hashimoto and Possingham, 1989). Plastids can be differentiated into specialized types to carry out specific functions depending on the tissue and organ types. Carotenoids are accumulated in almost all types of plastids, and are therefore found in abundance or at trace levels in most plant organs and tissues. Chromoplasts are present in flower tissues and fruits, and are responsible for storing large amounts of carotenoids (Kohler and Hanson, 2000). Chromoplasts of different plants may store different carotenoids. For instance, lycopene accumulates prominently in tomato fruit, whereas lutein in marigold flowers (Ben-Amotz and Fishler, 1998; Moehs et al., 2001). Carotenoids can also be stored in elaioplasts in oilseeds. Carotenoid production and storage in the seed is important for seed dormancy, ABA production and antioxidant systems (Tan et al., 2003; Calucci et al., 2004; Frey et al., 2012).

In some oilseed species such as *Arabidopsis* and canola (*Brassica napus*), elaioplasts are specialized to store lipids at high levels even to a higher range than amyloplasts (Shewmaker et al., 1999). In many species, such as *Arabidopsis*, pumpkin, sunflower and canola, lutein is the major carotenoid (Matus et al., 1993; Shewmaker et al., 1999; McGraw et al., 2001; Lindgren et al., 2003). During seed development, carotenoids can be stored as specialized lipoprotein-sequestering structures in elaioplasts (Vishnevetsky et al., 1999).

1.5 Small RNA and miRNA

Small RNAs (sRNA) are a class of RNA, 18-24 nucleotides long, that are not translated to protein but are major gene expression regulators at the post-transcriptional level (Bologna et al., 2012). Plant sRNA are classified into various groups, such as small interfering RNA (siRNA), microRNA (miRNA), natural antisense siRNA and *trans-acting* siRNA (Chapman et al., 2007; Wei et al., 2012). MiRNAs function by cleaving target mRNA (Llave et al., 2002), transcriptional inhibition (Khraiwesh et al., 2010) or translational repression (Brodersen et al., 2008). MiRNA biogenesis starts with the transcription by RNA polymerase II in the nucleus. In plants, mature miRNA formation is a multi-step process (Bartel, 2004). First, pri-miRNA is cleaved to miRNA precursor with a characteristic hairpin structure. Then, pre-miRNA is further cleaved to a miRNA duplex (miRNA:miRNA), a short double-stranded RNA (dsRNA) and a mature miRNA (Bartel, 2004). Finally, mature miRNAs are predominantly incorporated into the RNA-induced silencing complex (RISC) in which they negatively regulate gene expression by inhibiting translation or degrading coding mRNAs by perfect or near-perfect complementation to target mRNAs (Rhoades et al., 2002). In plants miRNAs target mostly transcription factors (Mitsuda and Ohme, 2009), hormone receptors

(Navarro et al., 2006) and enzymes (Fujii et al., 2005). In *Arabidopsis*, approximately 300 miRNAs (<http://microrna.sanger.ac.uk>) have been identified and grouped into families containing members whose sequences differ by only a few nucleotides.

1.6 Role of *microRNA156* in Carotenoid Regulation

The microRNA156 (*miR156*) family in *Arabidopsis* has eight members (a-g) which regulate a network of genes by repressing 10 *SQUAMOSA PROMOTER BINDING PROTEIN LIKE* (*SPL*) genes, which encode plant-specific transcription factors (Wei et al., 2010). SPLs play important roles in several physiological processes, such as fruit development, flowering time, vegetative to reproductive phase transition (Arazi et al., 2005; Kropat et al., 2005) and secondary metabolism (Wei et al., 2010; Gou et al., 2011; Wei et al., 2012). SPL transcription factors have been identified in various plant species, including maize and *Arabidopsis* (Lannenpaa et al., 2004; Guo et al., 2008; Wang and Burge, 2008). SPL proteins contain a conserved DNA binding motif through which they bind to the specific sequence in the promoters of target genes and regulate their expression. Based on studies in *Arabidopsis* (Cardon et al., 1999; Liang et al., 2008), *Antirrhinum majus* (Klein et al., 1996) and *Chlamydomonas reinhardtii* (Kropat et al., 2005), the consensus SPL binding sequence was determined to be T(N)CGTACAA with the core sequence being GTAC (Wei et al., 2012). The *Arabidopsis* 16 SPL proteins have a conserved DNA binding domain (Cardon et al., 1997; Lannenpaa et al., 2004; Birkenbihl et al., 2005), but only 10 of them were determined to be regulated by miR156 (Rhoades et al., 2002; Schwab et al., 2005). Based on *in silico* analyses, SPL binding elements with a GTAC element invariant core were present in the promoter regions *CCD* and *NCED* genes. Interestingly, the promoter of *miR156b* also

contains SPL binding elements and is regulated by SPL15 in a feedback regulatory loop system (Wei et al., 2012).

In silico analysis revealed that only *SPL* genes have the segments complementary to the mature sequence of miR156 in the Arabidopsis genome (Rhoades et al., 2002). *MiR156* overexpression in Arabidopsis is accompanied by faster rosette leaf initiation, enhanced leaf number and delayed flowering. (Schwab et al., 2005). These characteristics are similar to *max3* and *max4*, which are defective in *CCD7* and *CCD8* functions, respectively (Sorefan et al., 2003; Booker et al., 2004). Since these two mutants showed a decrease in strigolactone accumulation, this suggests a link between carotenoid metabolism and *miR156* expression. In addition, *miR156* overexpression mutant showed an increase in the levels of zeaxanthin, β -carotene, violaxanthin and lutein (Wei et al., 2012), and overexpression of *miR156* in *Brassica napus* caused enhanced branching and increased accumulation of carotenoids (Wei et al., 2010). The various functions of SPLs have been reported (Cardon et al., 1997; Schwarz et al., 2008), and based on their roles, they were grouped into four categories *SPL9/SPL15*, *SPL6/SPL13*, *SPL11/SPL10/SPL2* and *SPL3/SPL4/SPL5* (Guo et al., 2008). *SPL3*, *SPL4* and *SPL5* are involved on plant juvenile-to-adult transition (Cardon et al., 1997; Wu et al., 2006). *SPL9* and *SPL15* are regulated vegetative phase transition and negatively regulate leaf initiation (Schwarz et al., 2008). *SPL11*, *SPL10*, and *SPL2* regulate morphological change and shoot maturation in the reproductive phase (Shikata et al., 2009). To investigate which *SPL* genes are the best candidates to regulate carotenoid biosynthesis, mutants of all *SPL* genes were studied (Wei et al., 2012). Of all the *spl* mutants, only *spl15* showed increases in levels of carotenoids, whereas other *spl* mutants were less affected (Wei et al., 2012). *SPL15* is active in the vegetative shoot apex; therefore, *spl15* mutant phenotypes were found to affect vegetative development, including juvenile-to-adult phase transition (Schwarz et al.,

2008). In addition, *SPL15* loss-of-function leads to enhanced branching, altered inflorescence architecture and shortened plastochron during vegetative growth (Schwarz et al., 2008). Mutation in the *miR156* target site of the *SPL15* gene leads to reduced *SPL15* transcript cleavage, and thereby increased accumulation of *SPL15* mRNA in the *Arabidopsis* mutant, and also promotes juvenile-to-adult phase change (Usami et al., 2009), but the exact mechanism of this effect is not yet well understood.

1.7 Proposed Research

Enhanced expression of *miR156* results in reduced *SPL15* expression, increased shoot branching and enhanced carotenoid content (Wei et al., 2010; Fu et al., 2012; Wei et al., 2012). An *Arabidopsis* mutant, *sk156*, isolated in our laboratory has enhanced *miR156* expression, carotenoid accumulation and shoots branching. These phenotypes of *sk156* are consistent with reduced levels of the branching inhibitors, strigolactones. Since strigolactones are carotenoid degradation products, the increased carotenoid accumulation in this mutant is likely due to reduced carotenoid degradation rather than increased carotenoid biosynthesis. This is supported by previous findings that none of the carotenoid biosynthesis genes were up-regulated in the *sk156* mutant, and by *in silico* analysis, which revealed that none of these genes had complementary sequences to the mature *miR156* sequence (Wei et al., 2012). Therefore, I hypothesize that the enhanced carotenoid content in *sk156* and *RS105* (a transgenic *miR156* overexpression line) may be due to reduced carotenoid degradation resulting in low levels of strigolactones and other carotenoid degradation products (apocarotenoids), and that *SPL15* functions by activating the expression of carotenoid degradation *CCD* and *NCED* genes. This is supported by my *in silico* analysis that revealed the existence of between two and eight SBD (*SPL* Binding Domain) invariant core GTAC

elements in the promoters of all *CCD* and *NCED* genes (except *CCD1*). Therefore, I set out to investigate whether expression of *CCD* and *NCED* genes is affected by changes in the expression of *miR156* and *SPL15*.

In addition, reports in the literature have shown cases where enhanced carotenoid accumulation was accompanied by changes in the anatomical structure of plastids resulting in enhanced ability to store carotenoids (Paolillo et al., 2004; Kolotilin et al., 2007; Galpaz et al., 2008; Cazzonelli and Pogson, 2010). Further analysis revealed changes in the thylakoid membranes of the plastids allowed them to store large quantities of carotenoids (Paolillo et al., 2004). Therefore, I analyzed the anatomical structure of plastids of seeds of different *Arabidopsis* lines by transmission electron microscopy (TEM).

I hypothesize that

- *SPL15* activates at least some of the *CCD* and *NCED* genes, and that suppression of *SPL15* by *miR156* leads to reduced expression of *CCD* and *NCED* genes, reduced carotenoid degradation, and hence enhanced carotenoid accumulation.
- Enhanced seed carotenoid accumulation may be associated with changes in the anatomical structure of the plastids allowing them to store excess carotenoids.

The objectives of this study are to:

- Determine if any of the *CCD* and *NCED* genes are regulated by *SPL15* by employing quantitative real time PCR (qRT-PCR) to test expression of the nine *CCD* and *NCED* genes in the siliques and roots of WT (Wild Type), *sk156* (*miR156* overexpression mutant), *RS105* (transgenic *miR156* overexpression line), *spl15* (*SPL15* knockout mutant) as well as in 35S:*SPL15* (*SPL15* overexpression line).
- Confirm whether *SPL15* binds to any of the GTAC elements in the nine *CCD/NCED* genes using ChIP-qPCR.

- Analyze plastids of WT, *sk156*, *RS105* by transmission electron microscopy to determine the impact of *miR156* overexpression on anatomical structure.

2 MATERIAL AND METHODS

2.1 Plant Materials and Growth Conditions

All the *A. thaliana* lines used in this work were in the Columbia background. Seeds of *sk156* (*miR156* overexpression mutant), *RS105* (transgenic *miR156* overexpression line), 35S:SPL15 (SPL15 overexpression lines), *spl15* (SPL15 knock out mutant) and WT (wild type) were sown in soil in plastic pots and left in a 4°C cold room for two days before transfer to growth chambers. The *miR156* over expression mutant (*sk156*) was selected from an *Arabidopsis* activation-tagged population that was developed using a T-DNA construct containing four repeats of the enhancer element of the cauliflower mosaic virus (CaMV) (Wei et al., 2012). The *SPL15* knock out mutant, SALK_138712, was used as a *spl15*. The *RS105* was kindly provided by Dr. Gang Wu (Wu et al., 2009). The 35S:SPL15 lines were generated in our lab. The seeds were germinated and seedlings grown under 16 hours of light and 8 hours of dark conditions in soil. Siliques were used at 10 DPA (days post anthesis) for expression analysis, because this is the stage at which *miR156* is expressed at its highest level.

For seedlings grown on agar plates, seeds were surface-sterilized and sown on top of solid MS medium in petri dishes. After stratification for at least two days at 4°C in the dark, plates were placed under continuous fluorescent white light (photon fluence rate of 80 $\mu\text{mol m}^{-2} \text{sec}^{-1}$) at 22°C to induce germination. Roots were used for RNA extraction 10 days after seed germination.

2.2 RNA Extraction from Arabidopsis Tissue

Total RNA was extracted according to a modified MasterPure™ Plant RNA Purification Kit (Illumnia, Madison, USA). For this purpose, 15-20 siliques (25-50 mg) were ground to a fine powder using liquid nitrogen with a pre-chilled mortar and pestle. The extraction buffer (600 µl of lysis solution, 6 µl of 100 Mm DDT and 1 µl of proteinase k) was immediately added to each sample in a 1.5 ml tube and tissue was mixed for 1 min. The mixture was placed at 56° C for 15 min, and then centrifuged at 16000 g for 10 min at room temperature, and the supernatant was transferred to a new tube. In the second step, 250 µl of protein precipitation reagent was added to pellet and the mixture was centrifuged at 16000 g for 10 min at 4° C. The supernatant was transferred to a new tube and 750 µl of isopropanol was added to each tube and tubes were inverted 40-50 times then placed at -20° C for 10 min. Solutions were centrifuged at 15000 g for 10 min to pellet RNA. In the third step, 200 µl of DNase solution (173 µl RNase-free water, 20 µl 10X DNase buffer, RNase-free DNase and 2 µl RiboGuard RNase Inhibitor) was added to each tube and incubated at 37°C for 25 minutes to remove DNA contaminants. Afterwards, 200 µl of lysis solution and 200 µl of protein precipitant reagents were added to each sample and solutions were centrifuged at 13000 g for 10 min at 4° C. The Supernatant was transferred to a new tube and 750 µl of isopropanol was added to each tube and the mixture was centrifuged as in the previous step. The RNA pellet was washed twice with 70% ethanol, and then the RNA was dissolved in 40 µl of sterile ddH₂O.

2.3 DNA Extraction from Arabidopsis Tissues

Leaf tissue (200 mg) was ground with a plastic rod inside of a 1.5 ml tube, and 500 µl of extraction buffer (2% CTAB, 1.4 M NaCl, 20 mM EDTA and 100 mM Tris) was then added

to the ground sample. The mixture was mixed for 15 seconds by vortexing and then 500 μ l of chloroform was added to the tube and mixed. The mixture was centrifuged at 1000 g for 5 minutes, and the supernatant was transferred to a new tube. Afterwards, 750 μ l of isopropanol was added to the supernatant and centrifuged at 18000 g for 15 minutes. The supernatant was then discarded, and the pellet was washed with 70 % ethanol and allowed to dry. The dry pellet was dissolved in 30 μ l of sterile ddH₂O.

2.4 Preparation of Chemically Competent *E. coli* Cells

A colony from a freshly streaked *E. coli* (TOPO 10) was used to inoculate 5 ml of Luria Broth (LB), and incubated overnight with shaking at 37°C. Two mL of this starter culture was then used to inoculate 1 L of LB medium in a flask and allowed to grow at 37°C with shaking. OD₆₀₀ was measured on an hourly basis until it reached 0.35-0.4, and then the culture flask was placed on ice for 15 minutes. The culture was then transferred into the centrifuge bottles and centrifuged at 2700 g at 4°C for 10 min. The pellet was re-suspended in 20 ml of cold 0.1 M CaCl₂ and inoculated on ice for 30 min, and then centrifuged at 1700 g for 10 min at 4°C. The supernatant was discarded and cells were re-suspended in 1 ml of 0.1 M CaCl₂. The suspended cells were then transferred into a 50 ml tube and kept on ice for 3 h. To each 50 ml tube, 400 μ l of sterile 15% glycerol was added. The cells were divided into 40-50 μ l aliquots in sterile eppendorf tubes, flash frozen, and stored at -80°C until use.

2.5 Preparation of Electro-Competent *Agrobacterium tumefaciens* Cells

A single colony of *A. tumefaciens* (GV3101) was used to inoculate 5 ml of LB medium in a culture tube. The cultures were grown at 28°C with shaking overnight. A 3 ml aliquot of the

of starter culture was then used to inoculate 1 L of LB medium, which was allowed to grow at 28°C on a shaker until OD₆₀₀ reached 0.5-0.7. The culture was then transferred into centrifuge bottles and centrifuged at 1700 g at 4°C. The supernatant was discarded and the pellet re-suspended in 50 ml of sterile cold ddH₂O and centrifuged at 1700 g at 4°C for 10 min. The supernatant was again discarded and the pellet re-suspended in 15% glycerol. Cells were then harvested by centrifuging at 1700 g for 10 minutes at 4°C. Glycerol was decanted and an equal volume of ice-cold 15% glycerol was added. Cells were divided into 40-50 µl aliquots in eppendorf tubes, flash frozen, and stored at -80°C until use.

2.6 Plasmid Extraction

Bacterial colony containing pENTER-SPL15 was inoculated in 3 ml of LB broth (containing the appropriate antibiotic) in a culture tube. For kanamycin-resistant clones, kanamycin was added to LB media to a final concentration of 50 µg/ml. The tubes were put on a shaker at 40 g for 14-16 h at 37°C. The bacterial culture was then transferred to a 1.5 ml micro centrifuge tube, and then the bacterial cells were collected by centrifugation at 19300 g for one min. The supernatant phase was removed and the bacterial pellet was suspended in 200 µl of solution I (50 mM glucose, 25 mM Tris-HCl and 10 mM EDTA) and mixed well, then 200 µl of solution II [0.2 N NaOH and 1% (w/v) SDS to final volume of 10 ml] was added and tubes were inverted 8-10 times gently. Finally, 200 µl of solution III (5 mM CH₃COOK and 115 ml of Glacial acetic acid to a final volume of 100 ml) was added and tubes were inverted 8-10 times gently. Tubes were placed on ice for 5 minutes. Bacteria and protein debris were removed by centrifugation at 19300 g for 5 minutes, and the supernatant was transferred to a new tube. Subsequently, 1 ml of 100% ethanol was added to each tube and placed at -20°C

for 10 min. DNA was collected by centrifugation at 18000 g for 10 minutes. Ethanol was discarded and the pellet was washed with 70% ethanol. The pellet was then dissolved in 40 μ l of sterile ddH₂O.

2.7 DNA Sequencing

DNA of constructs and PCR products was analyzed by sequencing at the DNA sequencing facilities at Robarts Research Institute (Western University) and the Southern Crop Protection and Food Research Center, Agriculture and Agri-Food Canada, London, Ontario.

2.8 Primer Design

For testing the transcript level of *CCD/NCED* genes, the coding regions of genes were selected for designing the primers. These primers were used for subsequent cloning, sequencing and qPCR analysis. For the ChIP-qPCR, the promoter regions of *CCD/NCED* genes were used for designing the primers. All of the primers were designed using primer select Lasergene 10 software with the following parameters for those primers that were used for qPCR: product size ranged from 80-200 bp, primer length ranged from 20-25 bp and melting temperature between 58-65°C. The primers were aligned with Primer-Blast software (<http://www.ncbi.nlm.nih.gov/tools/primer-blast/>) (Table 3). All PCR amplification products were sequenced to ensure product identity.

2.9 Generating SPL15-GFP Fusion Constructs

To make the 35S:SPL15-GFP construct, the full CDS of *SPL15* (accession # AT3G57920) from leaf cDNA was amplified by PCR using SPL15-R1 and SPL15-F primers (Table 3) and High Fidelity DNA polymerase. For the *SPL15* C-Terminal fusion, four bases CACC were added to the forward primer and the stop codon was removed from the reverse primer (SPL15-R1 and SPL15-F; Table 3). Purified PCR products were sub-cloned into the pENTR/D-TOPO® vector. TOPO reaction was performed by adding 4 µl of PCR product, 1 µl of salt solution and 1 µl of vector, mixed and left in RT for 10 min then transferred to TOPO 10 chemically competent cells. After growth on an LB medium plate, which contained kanamycin, colonies were selected and cultured in an LB broth, and then the plasmid was extracted. Samples were confirmed by PCR and sequencing. Then the entry clones (pENTER/D-SPL15) were linearized by *Hpa I* and *PvuI* restriction enzymes, which each of them had one cutting site within the pENTER/D backbone but not within the *SPL15* cloned fragment. LR recombination was performed with Gateway compatible destination vector pMDC85 for SPL15 C-terminal fusion. LR recombination was performed between an *attL* site flanking the insert in the entry clone and an *aattR* site on the destination vector to generate an expression clone (Invitrogen). LR recombination was performed with 3 µl of entry clone containing 150 ng of DNA, 1 µl destination vector (100 ng DNA) and 1 µl of 5X LR Clonase Reaction Buffer. The reaction mixture was mixed by tapping and incubated at 25°C for 5 h. The reaction was terminated by adding 1 µl of proteinase K at and incubation at 37°C for 10 min. 2 µl of each LR reaction were transferred to TOPO 10 chemically competent cells then cultured on an LB plate containing kanamycin (50 µg/ml). Plasmids were extracted and confirmed by sequencing, *NcoI* enzyme digestion and PCR. The *NcoI* had one recognition site within pMDC85 vector and one recognition site within *SPL15* fragment.

The resulting expression vectors were introduced into *A. tumefaciens* GV3101 electro competent cells, which were then used to transform wild type Arabidopsis plants by the floral dip method (Zhang et al, 2006).

2.10 Arabidopsis Transformation

A. tumefaciens GV3101, harboring 35S::SPL15-GFP vectors was grown in LB broth supplemented with Rifampicin (25 µg/ml) and Kanamycin (50 µg/ml) at 28°C overnight. One ml of this feeder culture was used to inoculate 500 ml of LB broth containing Rifampicin (25 µg/ml) and Kanamycin (50 µg/ml). The culture was grown until the stationary phase (OD 1.4-1.8). *A. tumefaciens* cells were centrifuged at 1700 g for 10 min, and the pellet was suspended in 500 ml of 5% (w/v) sucrose solution, followed by the addition of 0.02% (v/v) Silwet L-77. Four-week old Arabidopsis plants were inverted and their aerial parts (inflorescences and axillary inflorescences) were dipped in the *A. tumefaciens* cell suspension for 10 sec. Dipped plants were then laid down and covered with a plastic cover for 16-20 h in dark conditions. Then the plastic cover was removed and the plants were transferred to a growth chamber, and they were allowed to grow to maturity. The seeds were then harvested and screened for transformants.

2.11 Screening for Arabidopsis Transformants

Seeds were surface sterilized using 250 ml of 70% ethanol containing 25 µl of triton X-100, for 10 min. The solution was then discarded and the seeds were washed with 95% ethanol for 20 sec. The seeds were sown on MS medium plate containing Hygromycin (25 µg/ml). After stratification for at least two days at 4°C in the dark, plates were placed under continuous

fluorescent white light (photon fluence rate of $80 \mu\text{mol m}^{-2} \text{sec}^{-1}$) at 22°C to induce germination. Transformants with true leaves and developed roots were transferred to soil in plastic pots, and the pots were covered with plastic and moved to the growth chamber under continuous fluorescent white light (photon fluence rate of $80 \mu\text{mol m}^{-2} \text{sec}^{-1}$) at 22°C . After 2 weeks, DNA was extracted from positive transformants, and then PCR was done with gene-specific primers to check the presence of the transgene. Expression of the transgene was evaluated by qRT-PCR.

2.12 Chromatin Immuno-Precipitation (ChIP)-qPCR

The ChIP assay was used to evaluate the interaction between SPL15 transcription factor on genomic DNA. The ChIP assay was performed according to the previously described protocol (Kwon et al, 2005; Gendrel et al, 2005), with some modifications. Three-week-old transgenic seedlings (400 mg) expressing SPL15-GFP was cross-linked with 1% formaldehyde solution under a vacuum (Scienceware®, Cat. # 420220000) for 15 min. Tissues were incubated with 0.125 M glycine under a vacuum for 5 min, then rinsed twice with 1X PBS and prepared for chromatin extraction. By using liquid nitrogen, tissues were ground to a fine powder and 10 ml of extraction buffer 1 (Table 2) was added to a 15 ml falcon tube and gently mixed. The solution was filtered via two layers of Miracloth into a 15 ml pre-chilled falcon tube. The solution was centrifuged at $5000 g$ at 4°C for 15 min (Eppendorf, Centrifuge 5810R). The supernatant was discarded and the pellet was re-suspended in 300 μl of extraction buffer 2 (Table 2). After centrifugation at $13,000 g$ for 10 min, the pellet was re-suspended in 100 μl of extraction buffer 3, layered on 400 μl of extraction buffer 3 (Table 2) and centrifuged at $16,000g$ for 1 h at 4°C . The pellet was re-

suspended in 100 μ l of nuclei lysis buffer (Table 2) by gentle pipetting and vortexing. The re-suspended chromatin solution was sonicated (Fisher Scientific, Sonic Dismembrator, model 100) four times for 15 s each at 10% power and between each sonication treatments, the sample was placed on ice for one min. The sonicated chromatin solution was centrifuged at 13,000 g for 5 min and the supernatant was transferred to a new tubes. The sheared chromatin solution was diluted to 1 ml in Dilution Buffer (Table 2). The chromatin solution was divided equally to three micro-centrifuge tubes and 40 μ l of Protein an agarose beads (Salmon Sperm DNA, Millipore, Cat # 16-157) was added to each tube and incubated for 1-2 h at 4°C. The beads were collected by centrifuge at 13,000 g for 30 s and 1000 μ l of pre-cleared chromatin solutions of each sample was subjected to five μ l of the anti-GFP antibody and incubated overnight at 4°C. The following day, 50 μ l of protein A- agarose beads were added to each tube and incubated at 4°C for 1h. The beads were recovered by centrifuge at 3800g at 4°C for 30 s. The immuno complexes were then washed with a low-Salt, high salt, LiCl Wash Buffer (Millipore, Cat # 20-156), and Tris-EDTA (TE) Buffer (Table 2) at 4°C for 5 min. After each step, the beads were collected by centrifuge at 3800g at 4°C for 30 s. After the last wash, the beads solutions were eluted in 200 μ l of fresh Elution Buffer. Cross-linking of the immuno complexes was reversed by incubation at 65°C overnight with 200 mM NaCl. On the third day, 2 μ l of proteinase K (40 ng), 20 μ l of 40 mM Tris-HCl (pH 6.5) and 10 μ l of 100 mM EDTA were added to each sample and incubated at 45°C for 1 h. The DNA was purified with phenol/chloroform (1:1; vol/vol) and precipitated with anhydrous ethanol, 0.3 M sodium acetate (NaOAc, PH 5.2) and 15 μ g of glycogen carrier. The DNA pellet was washed with 70% ethanol and re-suspended in 16 μ l of ddH₂O. Then the DNA was used to quantify specific regions of the promoter that may have SPL binding sequences using qPCR with promoter-specific primers (Table 2). For qPCR, 2 μ l of DNA, 1mM of each forward and

reverse primer, 5 μ l of PerfeCta® SYBR® Green FastMix® (Quanta Biosciences, cat# 95072-012) and 1 μ l of water were mixed and centrifuged briefly. The program suggested by the kit was used; i.e. 95°C for 35s (one cycle), then 94°C for 5s and 58°C for 30s (45 cycles) for quantitative amplification (Bio-Rad, CFX96™). Melt-curve analysis for each primer was performed according to the following steps (65-95°C for 5 s, with a 0.5°C increment). The relative amount of each region in the ChIP-DNA samples was normalized against % input DNA using the $2^{(-\Delta\Delta ct)}$ method (Bio-Rad, CFX96™). The relative amounts for each GTAC element in the promoter regions of candidate *CCD/NCED* genes in three different biological replicates were compared between each independent replicate and wild type plant as a control.

Table 1: The Buffers used in the ChIP assay

Buffers	Reagents amounts
Extraction Buffer 1	20 ml of 2M sucrose, 1 ml of 1M Tris-HCl (PH 8), 1 ml of 1 M Magnesium Chloride (MgCl ₂), 35µL OF 14.3 M β-mercaptoethanol (β-ME), 50 µL OF 0.2 M phenylmethylsulfonyl fluoride (PMSF), and two tablets of Protease inhibitor (PI) (Roche, Cat. # 04693132001) were added to the final volume of 100 ml Milli-Q water
Extraction Buffer 2	1.25 ml of 2 M sucrose, 100 µL OF 1 M Tris-HCl (pH 8), 100 µL of 1M MgCl ₂ , 0.5 ml of 20% Triton, 3.5 µl of 14.3 M β- mercaptoethanol, 5 µl of 0.2 M PMSF, and 1/5 of a complete tablet of PI were added to the final volume of 10 ml of Milli-Q water.
Extraction Buffer 3	8.5 ml of 2M sucrose, 100 µl of 1M Tris-HCl (pH 8), 75 µL of 20% Triton, 20 µl of 1 M MgCl ₂ , 3.5 µl of 14.3 M β-ME, 5 µL of 0.2 M PMSF, and 1/5 Complete tablet of PI were added to final volume of 10 ml Milli-Q water
Nuclei Lysis Buffer	0.5 ml of 1M Tris-HCl (pH 8), 200 µl of 0.5 M EDTA, 0.5 ml of 20% SDS and 1/5 of a complete tablet of PI were added to the final volume of 10 ml Milli-Q water.
ChIP Dilution Buffer	1.1 ml of 20 Triton, 48 µl of 0.5 M EDTA, 334 µl of 1 M Tris-HCl (pH 8), 668 µl of 5 M NaCL were added to the final volume of 20 ml Milli-Q water.
Low-Salt Immune Complex Wash Buffer	150 mM NaCl, 0.1% SDS, 1% Triton X-100, 2 mM EDTA, 20 mM Tris-HCl (pH 8)
High-Salt Immune Complex Wash Buffer	500 mM NaCl, 0.1% SDS, 1% Triton X-100, 2 mM EDTA, 20 mM Tris-HCl (pH 8)
TE Buffer	10 mM Tris-HCl (pH 8), 1 mM EDTA 1 M Tris-HCl (pH 6.5)
Elution Buffer	1 ml of 20% SDS, and 0.168 g of NaHCO ₃ were added to the final volume of 20 ml Milli-Q water.

2.13 Transmission Electron Microscopy

Arabidopsis seeds were dichotomized with a sharp razor and fixed in 2.5% glutaraldehyde and 1.6% paraformaldehyde in a sodium phosphate buffer pH 7.4 overnight, and then washed in Milli-Q water for 2-3 h. Seeds were post-fixed in 2% osmium tetroxide (OsO₄) for 2 h in the dark under the hood, then washed four times with Milli-Q water. Seeds were dehydrated in a graded acetone series, 20%, 50%, 70%, 90%, 95% and 100% followed by one exchange for 15-20 min for 20% until 95% and three exchanges for 100%. Pure plastic was prepared and seeds were infiltrated with it. To prepare pure plastic, 3.5 ml of Araldite, 4.5 ml of Epon 812, 18 ml of DDSA and 0.67 ml of 4-DM-30 were added together and mixed with a plastic rod. Seeds were immersed in 1:2 and 2:1 pure plastic: acetone and rotated gently on a mechanical wheel for 20 and 6 h respectively. Seeds were then immersed in pure plastic in flatbed embedding molds and polymerized at 65°C for 2 days. Specimens embedded in pure plastic were cut into 60 nm sections using an Ultracut E microtome equipped with a diamond knife (Diatome, Switzerland). Sections were transferred to copper grids (Cu-G400; EMS). Specimens were stained with 2% Uranyl acetate for 15 min and washed gently with Milli-Q water, then put on Reynold's lead citrate solution followed by a solid granule of NaOH for 1 min (Bozzola and Russell, 1992). Specimens were washed and air-dried, then observed with a Philips CM-10 transmission electron microscope operating at 60 kV. The Image J software was used to measure the size of the elaioplasts in the transmission electron micrographs according to the manufacturer's protocols (<http://rsbweb.nih.gov/ij/>). For each electron micrograph, the scale in Image J software was set based on the original scale which was provided with TEM, and then the area measurement was used to assess the elaioplasts sizes in sk156, RS105 and wild type.

2.14 Agarose Gel Electrophoresis

DNA and RNA fragments were separated in 1% agarose gel (W/V) prepared in a 0.5X TBE (Tris/Borate/EDTA) buffer. Gel Red (1.5 µg/mL) was added to the agarose gel before solidification. DNA and RNA samples were loaded with 1X loading dye and gel were run at 90 V.

2.15 Real Time-qPCR Analysis

Reverse transcription PCR was performed with 4 µl of 5X qScript cDNA SuperMix (Quanta Biosciences, US) with 900 ng of the RNA sample in a total volume of 20 µl. PCR was carried out according to company instructions (25° C for 5 min, 42° C for 30 min, and 85° C for 5 min). Samples were diluted four times by adding sterile ddH₂O. For qPCR, 2 µl of cDNA, 1mM of each forward and reverse primer, 5 µl of PerfeCta® SYBR® Green FastMix® (Quanta Biosciences, cat# 95072-012) and 1 µl of water were mixed and centrifuged briefly. The program suggested by the kit was used; i.e. 95°C for 35s (one cycle), then 94°C for 5s and 60°C for 35s (45 cycles) for quantitative amplification (Bio-Rad, CFX96™).

A number of reference genes, *PP2A3*, *ACTIN2*, *UBQ5*, and *UBQ10*, were assessed to select the best one for normalizing the qRT-PCR data. Since *UBQ10* gene showed the best target stability (M) value (M <0.5) among the *miR156* overexpression line and mutant, *spl15*, 35S:SPL15 lines and WT, it was chosen as a reference gene. The T-test was used to compare the relative transcript levels of each gene in each biological replicate among *miR156* overexpression line and mutant, *spl15*, 35S:SPL15 lines and WT.

Table 2: List of primer sequences that were used in this study

Name	Primer sequence	Product Size (bp)	Application
CCD1-Fq CCD1-Rq	TGTTCCGCGTGAGACAGCAG CCACCACTGCCACCGGTTTC	131	qRT-PCR for <i>CCD1</i>
CCD4-Fq CCD4-Rq	AAGATCTCCGGTGTGGTGAAGC CCGGATTACCAGGATCCCTAGC	133	qRT-PCR for <i>CCD4</i>
CCD7-Fq CCD7-Rq	CTAAACCGTGGCGACGACAA CCGGAAAATCTGACGGCTTG	130	qRT-PCR for <i>CCD7</i>
CCD8-Fq CCD8-Rq	CGTTTATGCATGCGGTGCTC GGTCGAGGCACGAAGAATGG	135	qRT-PCR for <i>CCD8</i>
NCED2-Fq NCED2-Rq	CCAACAGCTGGGCACCATTTAT GTCGACCCAATCGTTTTTCCTG	133	qRT-PCR for <i>NCED2</i>
NCED3-Fq NCED3-Rq	ATCTTCCGGTGGTCGGAAAACCT ATTTGACGGCGTGAACCATAACC	132	qRT-PC for <i>NCED3</i>
NCED5-Fq NCED5-Rq	TGTTACGACGAGGAGAGTTGG TATCCGCCGAATTCACGAAAGT	134	qRT-PCR for <i>NCED5</i>
NCED6-Fq NCED6-Rq	GAGCTGGGATCGGTCTAGTGGA TTGACCGTCGATCTTCACTTGG	131	qRT-PCR for <i>NCED6</i>
NCED9-Fq NCED9-Rq	GGAAAACGCCATGATCTCACA AGGATCCGCCGTTTTAGGAT	61	qRT-PCR for <i>NCED9</i>
SPL15-Fq SPL15-Rq	GGAAATCTGCTGGCTCCGAGA CAGCCACCGCCCATTTCAAC	150	qRT-PCR for <i>SPL15</i>
SPL15-F SPL15-R1	CACCATGGAGTTGTTAATGTGTTTCG AAGAGACCAATTGAAATGTTGAGGAG	1066	Cloning of <i>SPL15</i>
SPL15-F spl15-R2	CACCATGGAGTTGTTAATGTGTTTCG TCAAAGAGACCAATTGAAATGTTGAG	1069	Cloning of <i>SPL15</i>
GFP-F GFP-R	CAGTGGAGAGGGTGAAGGTG GGTAATGGTTGTCTGGTAAAAGG	515	Sequencing
SPL15-R	GAGCCGTTGTGGGTTGTGGTTTTCT		Sequencing
SPL15-F	GGCACCACAATGGGTGGATTTGAG		Sequencing
35S:F3	CAATCCCACTATCCTTCGCAAGACCC		Sequencing
Pro-CCD4-F1 pro-CCD4-R1	GCCGATTTCGATCATGGTTTA CGATCGGGGCTTACTTTTTTC	134	ChIP-qPCR
Pro-CCD4-F2 Pro-CCD4-R2	GCATGCATAACCCCAAAGAGTG TCATGGATGGTTCAGAGTTCAAAG	124	ChIP-qPCR
Pro-CCD4-F3	CAGACCAAGATTCCCATTTTAC	101	ChIP-qPCR

Pro-CCD4-R3	TGTACGGGGCATTCTAGCTACT		
Pro-CCD8- F1	AAGGCCATGTACTIONCAAACCAAT	179	ChIP-qPCR
Pro-CCD8- R1	CCAAGGTATTTTCATGATTGTTCA		
Pro-CCD8-F2	GAACAATCATGAAAATACCTTGGA	122	ChIP-qPCR
Pro-CCD8-R2	AAGTACGCATATCCTTGCAAAA		
Pro-CCD8-F3	TGCAAGGATATGCGTACTTGATAA	174	ChIP-qPCR
Pro-CCD8-R3	TCATCGTCCATTTAGAAAACCTCAA		
Pro-CCD8-F4	CTCTCGCCCAAAAACGAACG	157	ChIP-qPCR
Pro-CCD8-R4	TGAAAATGGCCAAAGCGTCG		
Pro-CCD8-F5	ACGCGTTGACAAAACAGAAA	151	ChIP-qPCR
Pro-CCD8-R5	CGTTCGCTTAAATTGGTGGT		
Pro-NCED5-F1	CTTTCGAGCTTCATATCAAACTT	83	ChIP-qPCR
Pro-NCED5-R1	AAGAACAGTTTACACGCATGTACTIONTA		
Pro-NCED5-F2	ATTTGCAGCTTACCGATTGAA	155	ChIP-qPCR
Pro-NCED5-R2	ACCAGGACCAGGTCTGTTTTT		
Pro-NCED6-F1	AATTGATTAGTAACTTTTGGGGACT	91	ChIP-qPCR
Pro-NCED6-R1	AAAATTCATGCGGTGTGTGA		
Pro-NCED6-F2	TTCACCAACGGTTACACACTIONTC	166	ChIP-qPCR
Pro-NCED6-R2	CAAAGTAATGGAAGAACGATAACTIONCTG		
Pro-NCED6-F3	ACATGTGTACACGGGCAAAA	80	ChIP-qPCR
Pro-NCED6-R3	ACAAAGTAATGGAAGAACGATAACTIONCTG		

3 RESULTS

3.1 Assessing the Specificity of DNA Fragments Amplified by PCR

The transcript levels of *CCD1*, *CCD4*, *CCD7*, *CCD8*, *NCED2*, *NCED3*, *NCED5*, *NCED6*, and *NCED9* genes were quantified using qRT-PCR. To confirm the specificity of the primers, the PCR products generated using each pair of primers were sequenced, and the sequences were subjected to a blast search at “*blast.ncbi.nlm.nih.gov/*” to determine the specificity of the PCR products. The results of the blast search revealed that the sequence of each fragment was 100% identical to its predicted original sequence (Appendix 1).

3.2 Analysis of *CCD/NCED* Expression in *miR156* Overexpression Plants

3.2.1 Effect of *miR156* on *CCD/NCED* transcript levels in roots

To assess the expression levels of *CCD* and *NCED* genes when *miR156* was overexpressed, qRT-PCR was performed using primers designed to amplify genes that were known to be involved in carotenoid catabolism: *CCD1*, *CCD4*, *CCD7*, *CCD8*, *NCED2*, *NCED3*, *NCED5*, *NCED6*, and *NCED9* (Fig 2). My hypothesis is that increasing the level of *miR156* expression will suppress expression of *SPL15* resulting in a lower level of *CCD/NCED* expression. The roots from 10 day-old seedlings were used to evaluate the expression of four *CCD* and five *NCED* genes. In experiments using three biological and two technical replicates for each plant line, the expression levels of *CCD4*, *CCD7* and *CCD8*, *NCED2*, *NCED6* and *NCED9* were found to be significantly lower in *sk156* and *RS105* than in wild type. The transcript level of *NCED3* was significantly lower in *sk156*, but was not affected in *RS105*. Expression of both *CCD1* and *NCED5* was unaffected in both *sk156* and *RS105* relative to wild type (Fig 2).

3.2.2 Effect of *miR156* on *CCD/NCED* transcript levels in siliques

The transcript levels of *CCD1*, *CCD4*, *CCD7*, *CCD8*, *NCED2*, *NCED3*, *NCED5*, *NCED6* and *NCED9* were also evaluated in siliques at 10 DPA (day post anthesis) in wild type, *sk156* and *RS105* (Fig 3). This experiment was conducted using three biological replicates and two technical replicates for each plant line. The transcript levels of *CCD7*, *NCED2*, *NCED3*, *NCED5* and *NCED9* were significantly lower compared to wild type. In contrast to the roots, *NCED5* was affected in both *RS105* and *sk156*. The transcript levels of *CCD1*, *CCD4*, *CCD8* and *NCED6* were not significantly affected in both *RS105* and *sk156*, and also the transcript levels of *CCD1* and *NCED6* were slightly higher in *RS105* and *sk156* compared to wild type (Fig 3).

The transcript levels of six *CCD/NCED* genes (*CCD4*, *CCD7*, *CCD8*, *NCED2*, *NCED6* and *NCED9*) in the root and five *CCD/NCED* genes (*CCD7*, *NCED2*, *NCED3*, *NCED5* and *NCED9*) in siliques were significantly lower in both *sk156* and *RS105* in comparison to the wild type. The *sk156* and *RSO75* showed significant decreases in the transcript levels of *CCD7*, *NCED2* and *NCED9* in both the roots and siliques. My results confirm my hypothesis that suppression of *SPL15* by *miR156* leads to a reduction in the expression of some *CCD* genes, and thus increased carotenoid accumulation in *miR156* overexpression lines.

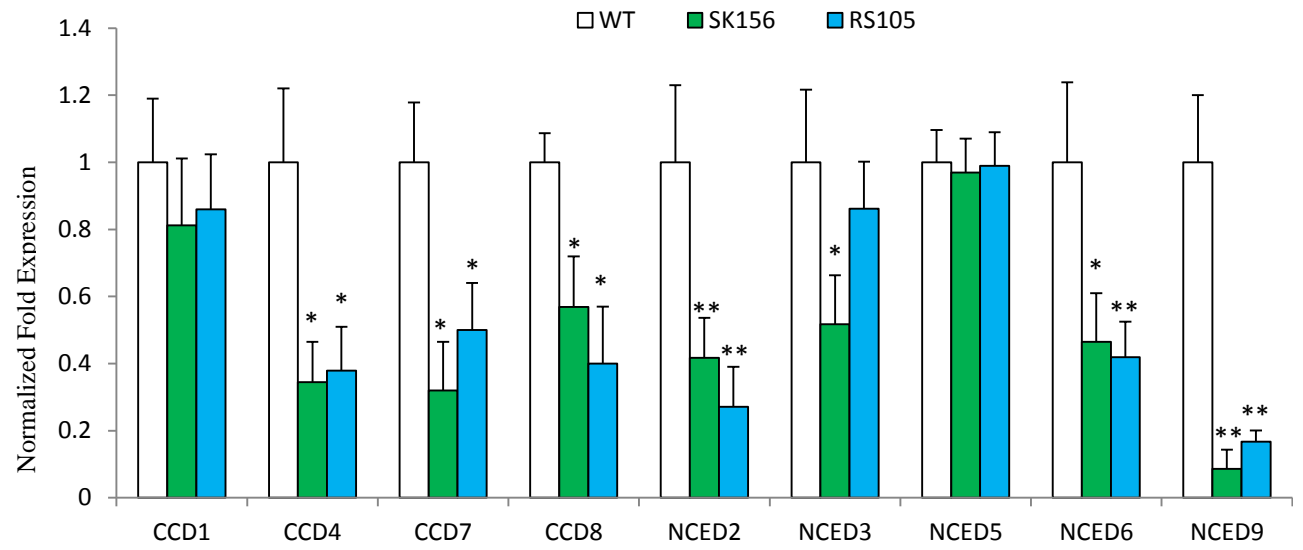


Figure 2. Transcript levels of *CCD* and *NCED* genes in the roots of 10 day-old seedlings of WT, *sk156* and *RS105* *Arabidopsis* plants.

The normalized relative transcript levels of *CCD* (carotenoid cleavage dioxygenase) and *NCED* (9-cis epoxy-carotenoid dioxygenase) genes obtained by q-RT-PCR, in the *sk156* (*miR156* overexpression mutant) and *RS105* (transgenic *miR156* overexpression line) compared to wild type. Roots were used 10 days after seed germination in MS medium. Data are the mean of six replicates: three biological replicates each replicated with two technical replicates. Error bars represent the standard error of three biological replicates. The asterisks represent a significant difference between the transcript levels in *sk156* and *RS105* plants relative to wild type using Student's t-test. * represents $P < 0.05$; ** $P < 0.01$.

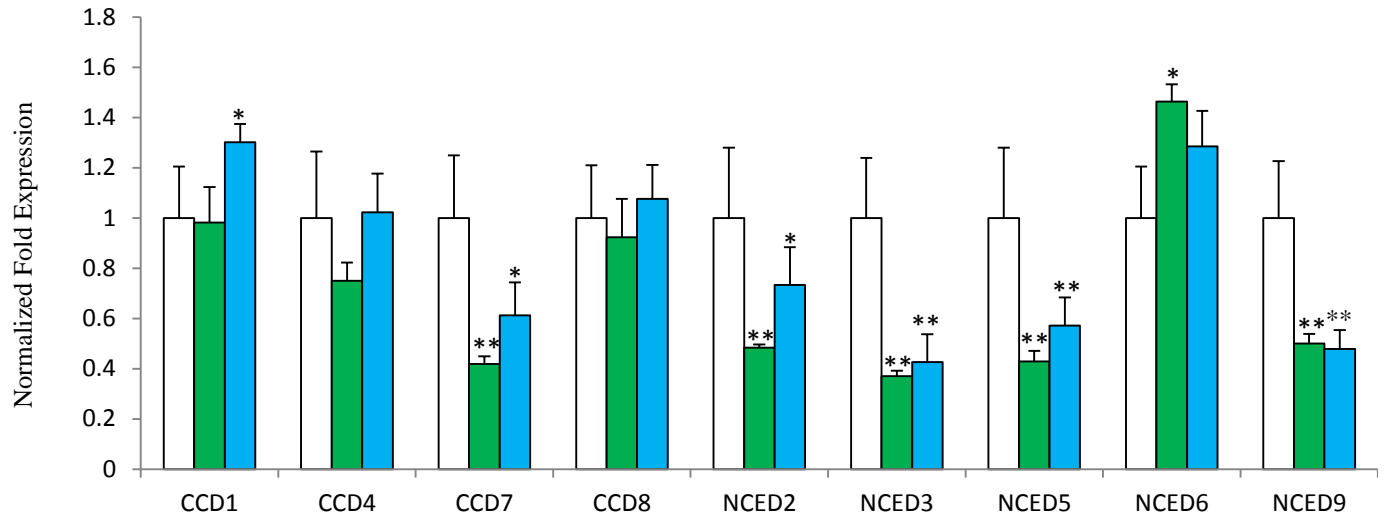


Figure 3. Transcript levels of *CCD* and *NCED* genes in 10 DPA (day post anthesis) siliques of WT, *sk156* and *RS105* *Arabidopsis* plants.

The normalized relative transcript levels of *CCD* (carotenoid cleavage dioxygenase) and *NCED* (9-cis epoxy-carotenoid dioxygenase) genes obtained by q-RT-PCR, in the *sk156* (*miR156* overexpression mutant) and *RS105* (transgenic *miR156* overexpression line) in comparison to the wild type (wild type values were set to an arbitrary number of 1). Data are the mean of six replicates: three biological replicates each replicated with two technical replicates. Error bars represent the standard error of three biological replicates. The asterisks represent a significant difference between the transcript levels in *sk156* and *RS105* plants relative to wild type using Student's t-test. * represents $P < 0.05$; ** $P < 0.01$.

3.3 Analysis of the Effect of SPL15 on the Expression of CCD/NCED Genes

Prior to conducting analysis of *CCD/NCED* expression, I investigated expression of *SPL15* in the *sk156*, *RS105*, 35S:*SPL15* (*SPL15* overexpression line) and *spl15* (*SPL15* knock out mutant), by qRT-PCR using *SPL15*- primers (*SPL15* Fq and *SPL15* Rq; Table 3). The *SPL15* PCR product was sequenced and then the sequence was subjected to a blast search (blast.ncbi.nlm.nih.gov/). The blast result showed that there was only one match for the *SPL15* PCR product and also it was 100% identical to the original *SPL15* sequence (Appendix 1) demonstrating that the primers were gene-specific. The transcript level of *SPL15* in the 35S:*SPL15*-2 line in both the roots and siliques was significantly higher in comparison to wild type (Fig 4). Although both 35S:*SPL15* lines showed higher transcript levels of *SPL15* than other lines, the transcript level of *SPL15* in 35S:*SPL15*-2 line was significantly higher than the 35S:*SPL15*-5 line in both the roots and siliques. In the roots, the transcript level of *SPL15* in *RS105* was significantly lower than wild type and also *sk156* showed a lower transcript level for *SPL15* than wild type (Fig 4A). In the siliques, the transcript level of *SPL15* in *sk156* was significantly lower than in the wild type and *RS105* showed a lower transcript level compared to wild type (Fig. 4B). As expected, the transcript level of *SPL15* in *spl15* was the lowest in both the roots and siliques and was significantly lower than in wild type.

3.3.1 Effect of SPL15 on transcript levels of CCD/NCED genes in roots and siliques

To assess expression of *CCD* and *NCED* genes in 10 day-old roots of 35S:*SPL15* lines and *spl15* (*SPL15* knockout) mutant, qRT-PCR was performed using primers specific to *CCD1*, *CCD4*, *CCD7*, *CCD8*, *NCED2*, *NCED3*, *NCED5*, *NCED6*, and *NCED9* (Table 2; Fig 5).

This experiment was conducted using three biological and two technical replicates for each plant line. The transcript levels of all *CCD/NCED* genes were significantly lower in *spl15* compared to wild type. In 35S:SPL15-2, except for *NCED3* and *NCED5*, the transcript levels of other *CCD/NCED* genes were significantly lower than in wild type, and also *NCED3* and *NCED5* were unaffected. The transcript levels of *CCD8* and *NCED5* in 35S:SPL15-5 were significantly higher than in wild type; however, the transcript levels of other *CCD/NCED* genes were unaffected (Fig 5).

3.3.2 The effect of SPL15 on expression of *CCD/NCED* genes in siliques

The transcript levels of *CCD1*, *CCD4*, *CCD7*, *CCD8*, *NCED2*, *NCED3*, *NCED5*, *NCED6* and *NCED9* were also evaluated in siliques at 10 DPA in the 35S:SPL15 lines and *spl15* (Fig 6). This experiment was conducted using three biological and two technical replicates for each plant line. Except for *CCD1* and *NCED6*, the transcript levels of other *CCD/NCED* genes were significantly lower in *spl15* mutant than in wild type. *NCED6* transcript was at its highest level in 35S:SPL15-2, but the transcripts of *CCD4*, *CCD7*, *CCD8* and *NCED2* were unaffected in the siliques of this line. In addition, the transcript levels of *NCED3*, *NCED5* and *NCED9* were significantly lower in 35S:SPL15-2 compared to wild type. In the 35S:SPL15-5 line, the transcript levels of *CCD4* and *NCED6* were significantly higher than in wild type. The transcript levels of other *CCD/NCED* genes were either unaffected or lower than in wild type. Levels of *NCED6* transcript were higher in both 35S:SPL15-2 and 35S:SPL15-5 compared to wild type.

3.3.3 The link between number of GTAC element and *CCD/NCED* transcript levels

In silico analysis showed the existence of GTAC elements in the promoter regions (1550 bp from first ATG) of all *CCD/NCED* genes, except for *CCD1* (Fig 7). GTAC was identified as the core sequence in the SPL binding site in promoters of genes regulated by SPL transcription factors (Wei et al, 2012). The numbers of GTAC elements vary among *CCD/NCED* promoters (Fig 7). Based on the effect of SPL15 on transcript levels of *CCD/NCED* genes, *CCD4*, *CCD8*, *NCED5* and *NCED6* showed significantly higher transcript levels in 35S:SPL15 lines compared to wild type. The number of GTAC elements in the promoter region of *CCD4*, *CCD8*, *NCED5* and *NCED6* are 3, 4, 2 and 3 respectively, and also the number of GTAC element in the promoter region of *CCD7*, *NCED2*, *NCED3* and *NCED9* are 4, 5, 4 and 8 respectively (Fig 7). Although the number of GTAC element in *CCD7*, *NCED2*, *NCED3* and *NCED9* are more than these numbers in *CCD4*, *CCD8*, *NCED5* and *NCED6*, the result showed that only the ones with lower numbers of GTAC elements were affected by *SPL15*.

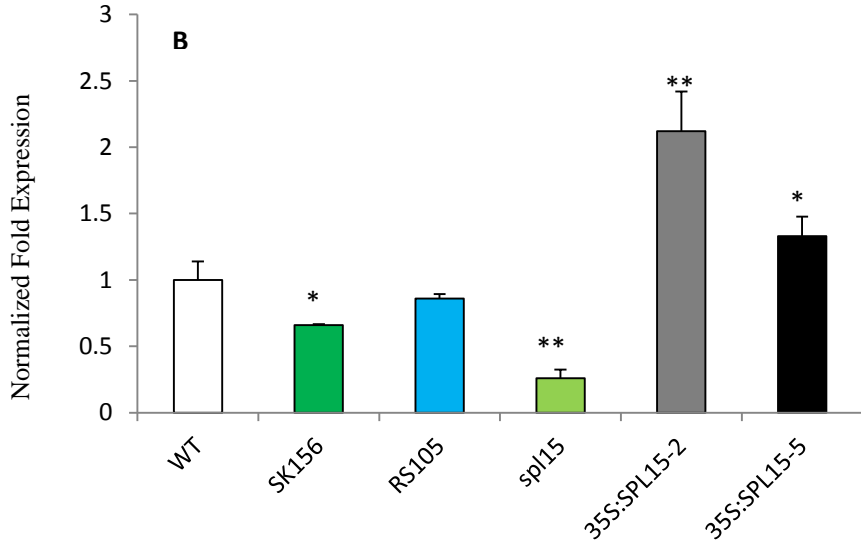
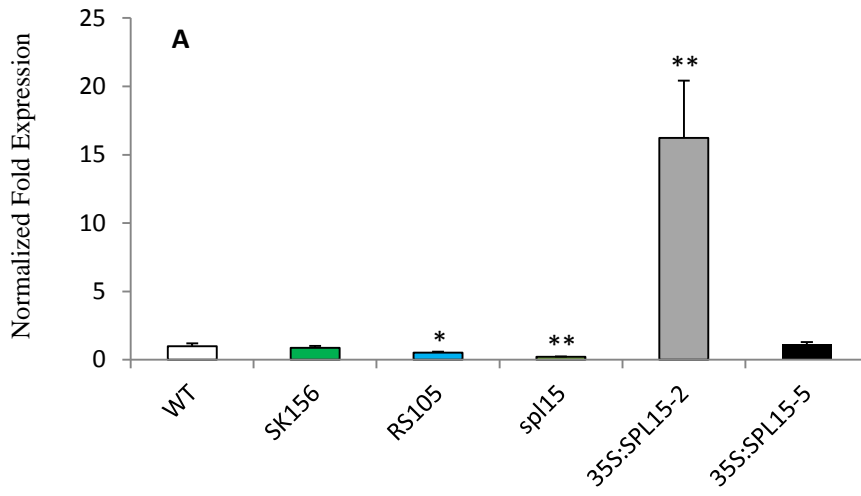


Figure 4. Transcript levels of *SPL15* in roots of 10 day-old seedlings (A) and 10 DPA (day post anthesis) siliques (B) of WT, *sk156* and *RS105*, *spl15* and 35S:*SPL15* Arabidopsis plants.

Normalized relative transcript levels of *SPL15* obtained by q-RT-PCR in *sk156*, *RS105*, *spl15* and 35S:*SPL15* compared to wild type. Data are the mean of three independent biological replicates and two technical replicates. Error bars represent the standard error of three biological replicates. The asterisks represent a significant difference among the transcript levels of *sk156* and *RS105*, *spl15* and 35S:*SPL15* plants to wild type using Student's t-test. * $P < 0.05$; ** represents $P < 0.01$.

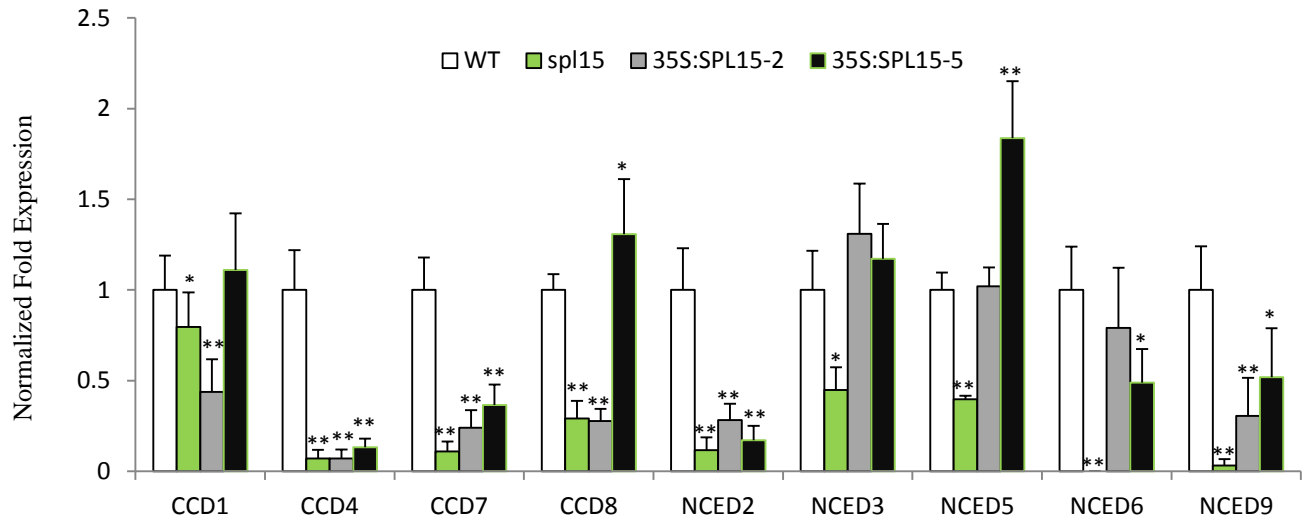


Figure 5. Transcript levels of *CCD* and *NCED* genes in roots of 10 day-old seedlings of WT, *spl15* and 35S:SPL15 *Arabidopsis* plants.

Normalized relative transcript levels of *CCD* and *NCED* genes obtained by q-RT-PCR in *spl15* and two 35S:SPL15 (*SPL15* overexpression lines) in comparison to wild type. Roots were used 10 days after seed germination in MS medium. Data are the mean of six replicates: three biological replicates each replicated with two technical replicates. Error bars represent the standard error of three biological replicates. The asterisks represent a significant difference among the transcript levels of *SPL15* in *spl15* and two 35S:SPL15 lines plants to wild type using Student's t-test.* represents $P < 0.05$; ** $P < 0.01$.

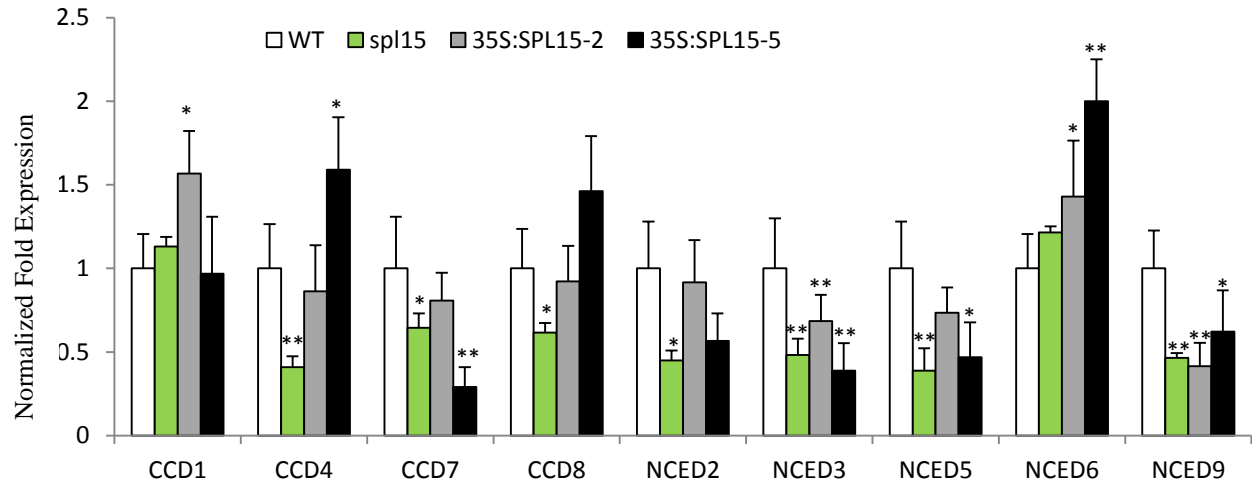


Figure 6. Transcript levels of *CCD* and *NCED* genes in 10 DPA siliques of WT, *spl15* and 35S:SPL15 Arabidopsis plants.

Normalized relative transcript levels of *CCD* and *NCED* genes obtained by q-RT-PCR in *spl15* and two 35S:SPL15 compared to wild type. Roots were used 10 days after seed germination in MS medium. Data are the mean of six replicates: three biological replicates each replicated with two technical replicates. Error bars represent the standard error of three biological replicates. The asterisks represent a significant difference among the transcript levels of SPL15 in *spl15* and two 35S:SPL15 lines plants to wild type using Student's t-test. * $P < 0.05$; ** represents $P < 0.01$

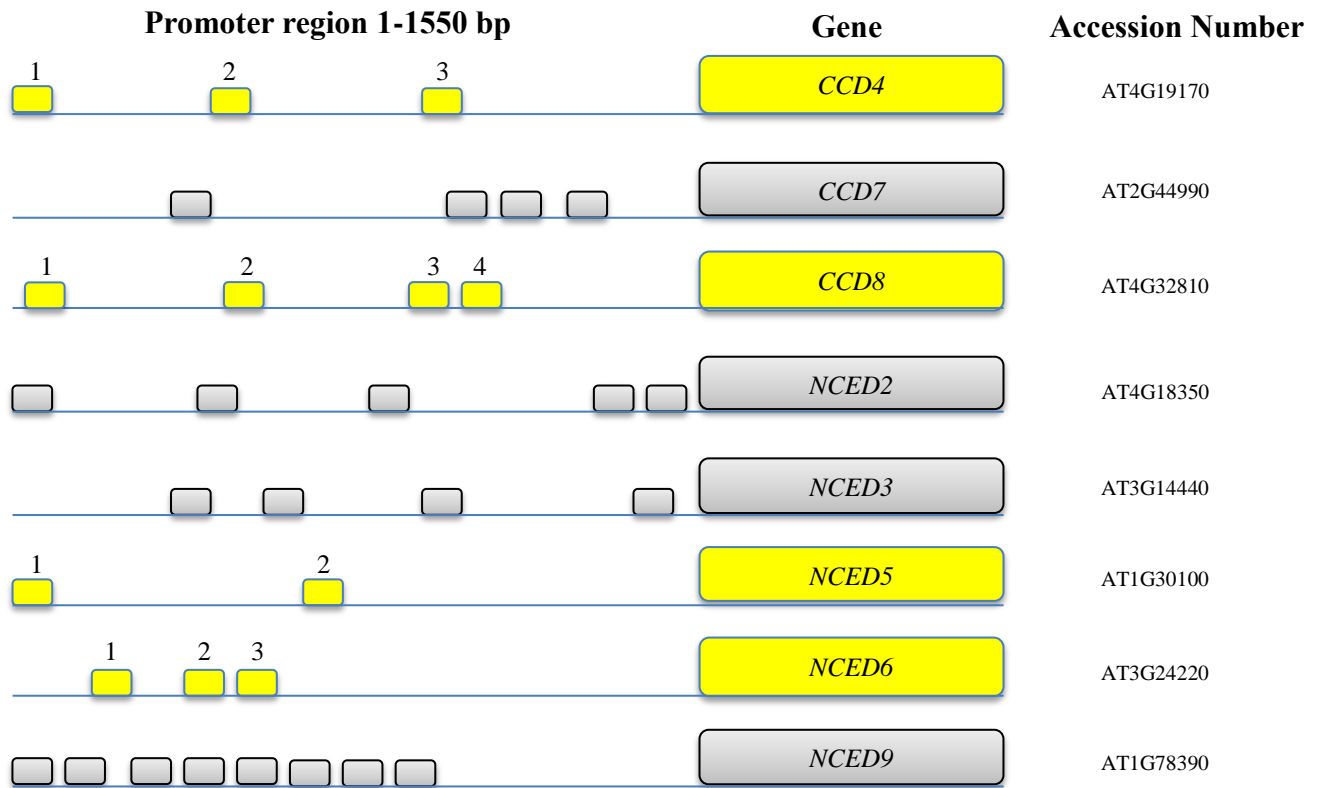


Figure 7. Schematic representation of the positions of GTAC elements in the promoter regions of *CCD* and *NCED* genes.

CCDI is not included due to lack of GTAC elements in its promoter. The genes whose transcripts were affected by SPL15 are shown in yellow. Small squares represent GTAC elements. Number 1, 2, 3 and 4 represent the positions of GTAC elements in the promoter regions of affected *CCD* and *NCED* genes.

3.4 Analysis of SPL15 Binding to Promoters of *CCD/NCED* Genes

I used ChIP-qPCR assays to test for the binding of SPL15 to putative SPL binding elements in the promoters of *CCD/NCED* genes. To that end, the SPL15-GFP construct (Fig 8), driven by a 35S promoter was introduced into Arabidopsis wild type plants using the floral dip method. After germination of T1 seeds on Hygromycin selective media, putative positive plants which showed long roots and true leaves were transferred into soil, and were then tested for the presence and expression of the transgene by PCR and qRT-PCR, respectively (Fig 9). Line 2, 3 and 5, which showed the highest transcript levels of *SPL15*, and wild type (control) were subjected to ChIP-qPCR assay using antibodies against the GFP protein. The ability of SPL15 to bind to putative GTAC elements in the promoter regions of candidate *CCD/NCED* genes (*CCD4*, *CCD8*, *NCED5* and *NCED6*; Fig. 7) which had already shown high transcript levels in the 35S:SPL15 lines relative to wild type) were investigated by ChIP-qPCR. To test SPL15 occupancy on genomic DNA, specific primers spanning each potential SPL15 binding element that contains GTAC core sequence (Fig. 7) were designed and used. The results are presented in Figure 10 and reveal strong occupancy by SPL15 of the promoter regions of some *CCD/NCED* genes. Of three binding sites in the promoter region of *CCD4* (Fig. 7), position 2 showed the highest occupancy by SPL15 in all three independent lines. Of the four putative SPL binding sites in the promoter region of *CCD8*, positions 1, 3 and 4 showed high occupancy by SPL15. Both binding sites in the promoter region of *NCED5* showed occupancy by SPL15. Line 3 showed the highest occupancy by SPL15 in the first binding site in *NCED5* promoter. For *NCED6*, all three lines showed occupancy by SPL15 in the binding sites 1 and 2. My results also revealed that SPL15 did not bind to positions 1 and 3 in *CCD4* promoter, position 2 in *CCD8* promoter and position 3 in *NCED6* promoter (Fig. 10). To test SPL15 selective binding, one pair of primers were

designed based on GTAC element in the promoter regions of *CCD7*, which was not affected by SPL15 in expression analysis (Fig. 5, 6). The result showed lower occupancy of SPL15 on the GTAC element in *CCD7* promoter compared to GTAC elements in the promoter regions of other affected *CCD/NCED* genes.

After finding high and selective binding of SPL15 to the promoter regions of affected *CCD/NCED* genes, I compared the consensus sequences in the vicinity of core GTAC elements from those which showed strong binding and those that showed weak or no binding to SPL15 by weblogo (<http://weblogo.berkeley.edu/logo.cgi>) (Fig 11). In the downstream of GTAC core in the promoter regions of affected GTAC elements between 10-18th position, the frequency of thymine (T) were dominant; however in the same region for those GTAC elements which showed weak or no binding, the frequency of adenine (A) were dominant (Fig 11). Interestingly, the upstream regions of GTAC elements not affected by SPL15, all the sequences at 10th and 15th positions (indicated by numbers 11 and 6 in figure 11) were A and T, respectively.



Figure 8. Map of the SPL15-GFP fusion construct.

From right to left: LB, Left border; 35S: Cauliflower mosaic virus 35S promoter; SPL15, the coding region of SPL15 without the stop codon; GFP, green fluorescent protein; Hyg, Hygromycin resistance gene; RB, Right border.

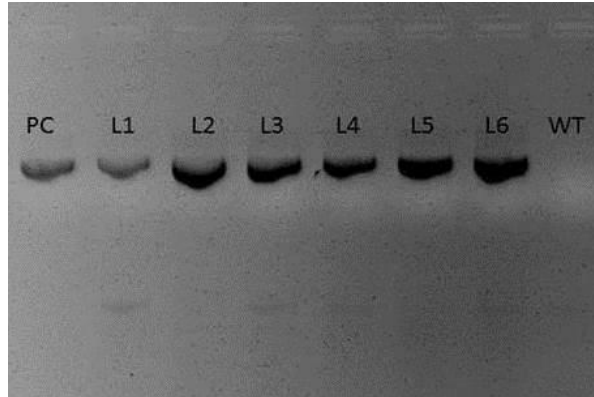
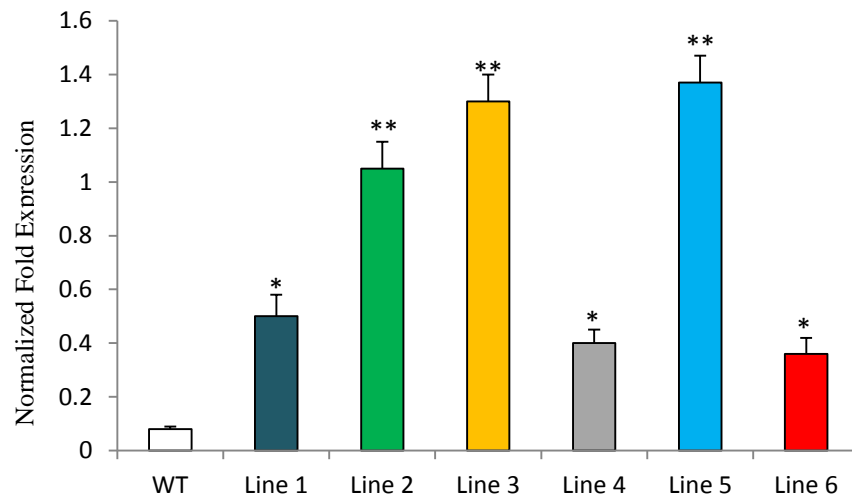
A**B**

Figure 9. PCR amplification of the *SPL15*+GFP fragment in different transgenic 35S:*SPL15*-GFP Arabidopsis lines (A); RT-qPCR analysis of *SPL15* transcript in the same transgenic lines (B).

PC, Positive Control (pMDC85 which harbors *SPL15*); L 1-6, Six independent transgenic lines. To amplify these fragments the *SPL15* forward primer and GFP reverse primer were used. B. The normalized relative transcript level of *SPL15* gene region obtained by q-RT-PCR, in six independent transgenic lines. Data for each line is the mean of three technical replicates. The asterisks represent a significant difference among the transcript levels of each transgenic line to wild type using Student's t-test. * $P < 0.05$; ** represents $P < 0.01$.

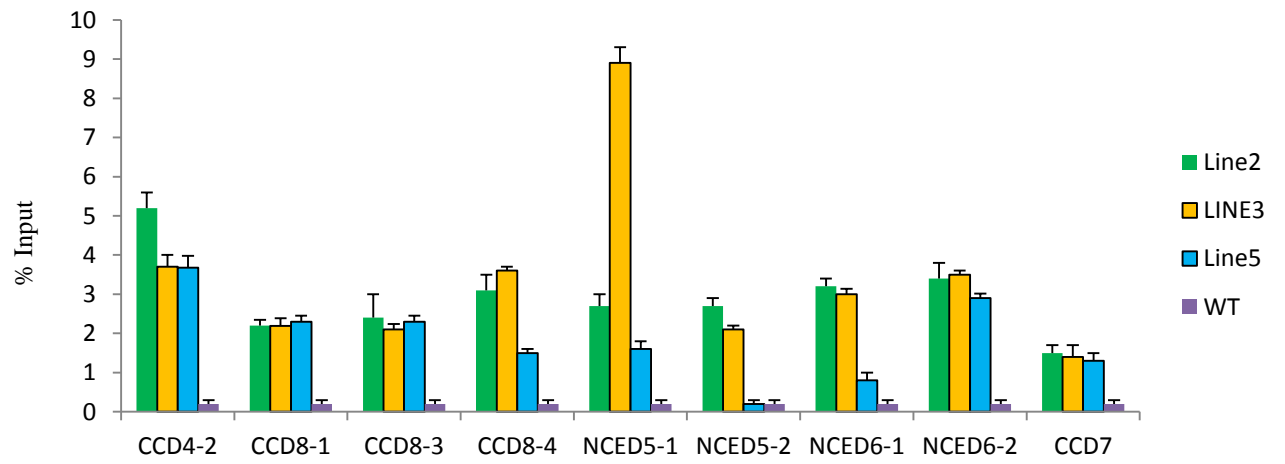


Figure 10. qPCR analysis of DNA generated from ChIP analysis of 35S:SPL15-GFP lines using anti-GFP antibody.

Bar graph shows the SPL15 occupancy on the promoter region of *CCD/NCED* genes. Data are normalized using input DNA. Data are the mean of two technical replicates. The numbers after gene name represent the position of GTAC element in the promoter regions of related genes.

Figure 11. Consensus sequences in the vicinity of core GTAC elements in *CCD/NCED* promoters showing strong binding (A) and weak or no binding (B) to SPL15

The letter G, T, A and C represent guanine, thymine, adenine and cytosine respectively. The level of conservation is shown by height of the letters.

3.5 Effect of MiR156 on the Anatomical Structure of Seed Elaioplasts

To determine if miR156 has an effect on the number and anatomical structure of plastids, I used transmission electron microscopy (TEM) to investigate plastids (elaioplasts) in the mature seeds of *sk156*, *RS105* and wild type plants. This experiment was carried out to determine whether the increase in seed carotenoid content of *sk156* mutant (Wei et al., 2012) was due to an increase in the carotenoid storage capacity of the cell as observed in other high carotenoid plant mutants (Paolillo et al., 2004). Since the seed cortex prevents OsO_4 absorption, the seeds were dichotomized to allow OsO_4 absorption for fixation and staining. Visual observation of electron micrographs of elaioplasts from *sk156*, *RS105* and wild type revealed that the former two had enlarged elaioplasts compared to wild type (Fig 12). In plants, plastoglobules are lipoprotein particles present in all types of plastids and accumulate carotenoids (Deruere et al., 1994). In elaioplasts of both *sk156* and *RS105* there was a trend towards larger size plastoglobules compared to wild type (Fig. 12). However, there was no significant difference between numbers of plastoglobules in elaioplasts of *sk156*, *RS105* and wild type. Due to the three dimensional structures of plastids in the plant cell and different cutting orientations of plastids when doing sectioning, comparing the size of few plastids was not a reliable approach to determine the effect of *miR156* on the anatomical structure of plastids. To account for these variations, the average size of 35 elaioplasts from each of *sk156*, *RS105* and wild type seeds were measured by Image j software (<http://rsbweb.nih.gov/ij/>). The results showed that the average elaioplasts size in *sk156* was significantly higher than the average of that in wild type. Although the average of elaioplast size in *RS105* was more than that in the wild type, the difference was not statistically significant (Fig 13). Thus, my results showed that the overexpression of *miR156*, which affected expression of *CCD/NCED* genes, further resulted in enlarged elaioplasts and

plastoglobules.

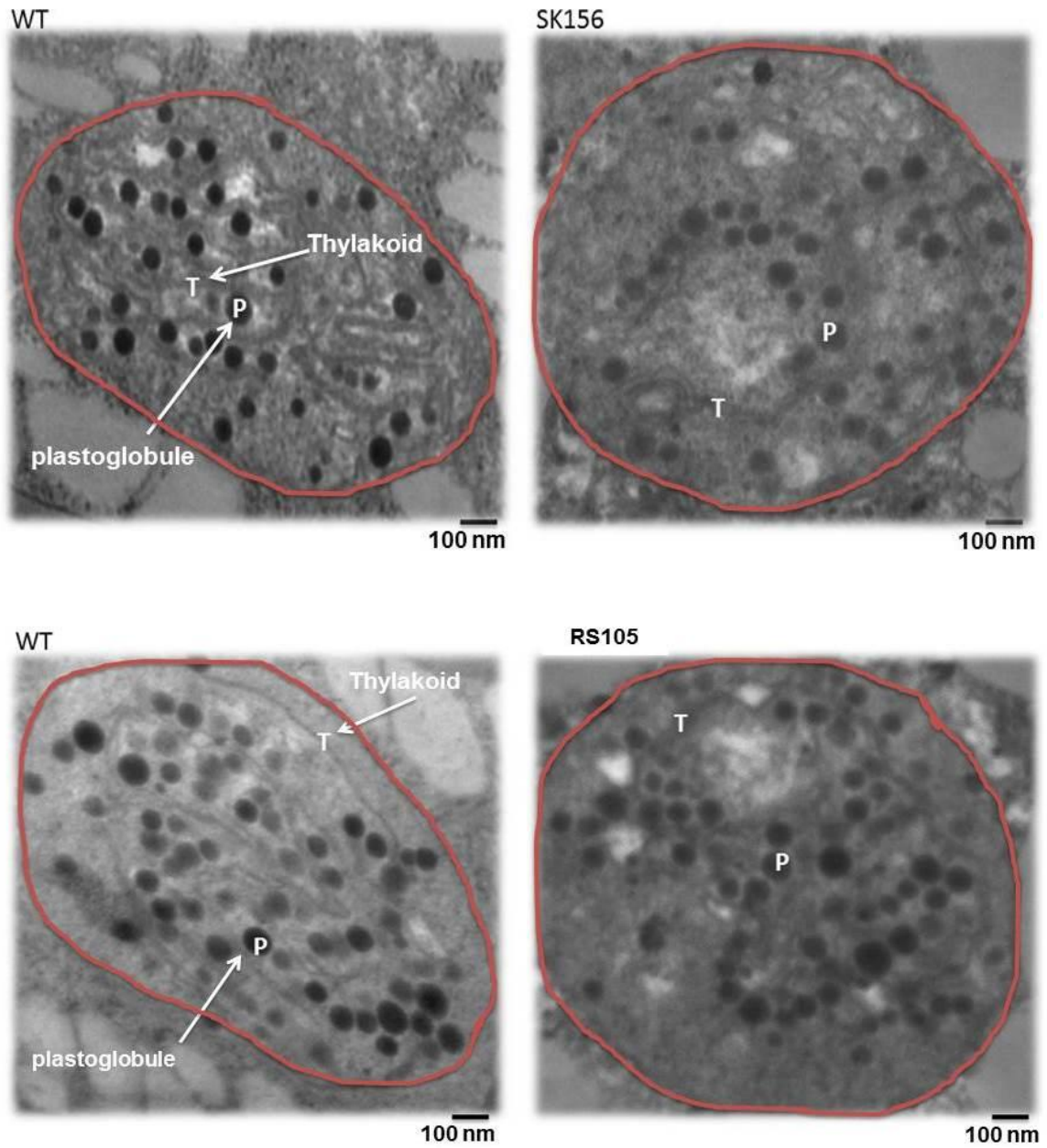


Figure 12. Transmission electron micrographs of Arabidopsis seed elaioplasts. *sk156*: *miR156* overexpression mutant, *RS105*: *miR156* overexpression line. P: plastoglobules, T: thylakoids. Scale bars: 100 nm. The red line represents the circumference of elaioplasts.

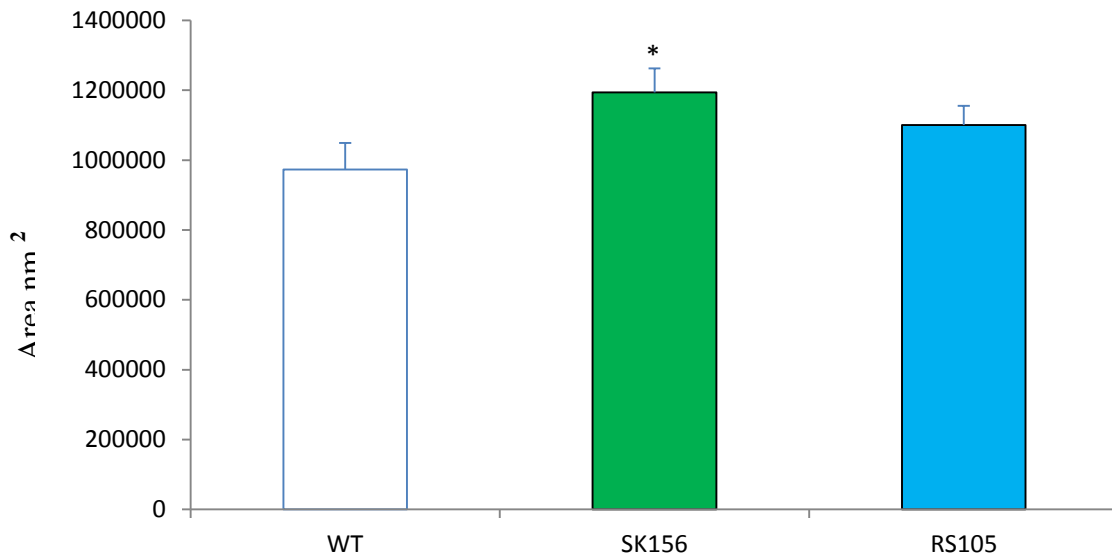


Figure 13. The averages size of 35 elaioplasts in mature seeds of *sk156*, *RS105* and wild type.

Error bars represent the standard error in the sizes of 35 elaioplasts. The asterisks represent a significant difference between the elaioplast size of *sk156* and *RS105* to wild type using Student's t-test. * $P < 0.05$.

4 DISCUSSION

4.1 Overview

Despite substantial progress in deciphering the carotenoid biosynthesis pathway (Ruiz-Sola and Rodriguez-Concepcion, 2012), significant gaps remain in understanding how carotenoid biosynthesis is regulated by developmental, temporal, spatial and environmental factors. This study was conducted to elucidate the mechanism by which *miR156* regulates carotenoid accumulation in Arabidopsis, and potentially in other plants. MiR156 family in Arabidopsis consists of eight members, which regulate a network of genes by repressing 10 *SPL* genes that encode plant-specific transcription factors (Rhoades et al., 2002; Gandikota et al., 2007). *In silico* analysis revealed that except for *SPL* genes, no other genes have complementary sequence to *miR156* in Arabidopsis (Rhoades et al., 2002). Among *SPL* genes which are targeted by *miR156*, *SPL15* was found to be the likely candidate involved in altered carotenoid levels in Arabidopsis seeds overexpressing miR156 (Wei et al., 2012). *SPL* proteins function by binding to promoters of genes that possess the consensus sequence T(N)CGTACAA, with GTAC element being the core sequence (Wei et al., 2012). In Arabidopsis, CCD and NCED enzymes are involved directly in carotenoid catabolism by oxidative cleavage of carotenoid molecules (Ruiz-Sola and Rodriguez-Concepcion, 2012). My *in silico* analysis of promoters of *CCD* and *NCED* genes revealed the existence GTAC elements in eight of the genes; *CCD1* being the exception. My hypothesis was that *SPL15* activates at least some of the *CCD/NCED* genes, and that suppression of *SPL15* by *miR156* leads to reduced *CCD* expression, reduced carotenoid catabolism, and hence enhanced carotenoid accumulation.

In this study, the molecular link between *miR156*, *SPL15* and *CCD/NCED* genes in the roots and siliques was assessed. In addition, since enhanced carotenoid level was shown in some

cases to be accompanied by increased plastid size (Paolillo et al., 2004), the effect of *mi156* on the anatomical structure and size of plastids in the seeds of *miR156* over expression line (*RS105*) and *sk156* mutant was investigated.

4.2 MiR156 Has a General Suppressive Effect on *CCD/NCED* Expression in Roots

Both *Arabidopsis* *sk156* and *RS105* plants are characterized by enhanced shoot branching and increased number of rosette leaves. The same phenotypes were observed in the *miR156* over expression plants of *Brassica napus* (Wei et al., 2010), switchgrass (Fu et al., 2012) and rice (Xie et al., 2012), which suggests that *miR156* function may be conserved in these species, and potentially in others as well.

In this study, overexpression of *miR156* showed varied effects on the transcript levels of *CCD/NCED* genes in siliques and roots. Not only was *CCD1* not affected in the siliques in *sk156*, its expression was in fact enhanced in *RS105* siliques compared to wild type (Fig 3). The same trend was observed in roots, where *CCD1* was unaffected (Fig 2). Among *CCD* genes, *CCD1* was the only member of this gene family unaffected in both siliques and roots. The *CCD1* is unique in its subcellular localization and activity (Ohmiya, 2009; Walter et al., 2010). Unlike other *CCD* and *NCED* proteins, which reside in the plastid, *CCD1* localizes to the cytoplasm (Strack et al, 2010). Moreover, unlike other *CCD/NCED* genes, my *in-silico* analysis revealed that the promoter of *CCD1* did not have the consensus GTAC element that is required for *SPL* binding, suggesting that it might not be regulated by *SPL15*.

CCD7 and *CCD8* are mainly expressed in roots and are involved in the biosynthesis of strigolactones, which are shoot branching inhibitory phytohormones (Booker et al, 2004;

Schwartz et al, 2004; Auldridge et al, 2006). Strigolactones are derived directly from carotenoids through the activities of *CCD* genes (Malusova et al, 2005). The result in this study revealed that the transcript levels of the *CCD7* and *CCD8* in the roots of *sk156* and *RS105* were significantly lower in comparison to the wild type. Some orthologous genes, such as *MAX3* in Arabidopsis, *RMS5* in pea (*Pisum sativum*), and *high tillering dwarf* (*HTD*) in rice (*Oryza sativa*), encode *CCD7* (Johnson et al, 2006; Booker et al, 2005; Zou et al, 2006), whereas *MAX4* in Arabidopsis, *RMS1* in pea, and *decreased apical dominance* (*DAD1*) in Petunia (*Petunia hybrid*) encode *CCD8* (Sorefan et al, 2003; Snowden et al, 2005; Arite et al, 2007). The mutants of these genes, *max3* and *max4*, *rms*, *htd* and *dad*, showed enhanced shoot branching (Turnbull et al, 2002; Johnson et al, 2006; Arite et al, 2007; Simons et al, 2007). Our findings showed that, enhanced *miR156* expression in both *sk156* and *RS105* reduced the expression of both *CCD7* and *CCD8* in the root; and this was accompanied by increased shoot branching and seed carotenoid levels. Despite high seed carotenoid content of *sk156*, the carotenoid biosynthesis genes were not up-regulated in this mutant, and these genes are not expected to be directly regulated by *miR156* because they do not possess *miR156*-related sequences (Wei et al, 2012). Thus, *miR156* may not have an effect on *de novo* carotenoid biosynthesis; however, since apocarotenoids, such as strigolactones, appear to be affected in *sk156* and *RS105*, an effect on carotenoid catabolism, and consequently *CCD* and *NCED* genes, is likely. The *sk156* and *RS105* plants are characterized by enhanced shoot branching, which is likely due to the decreased level of the shoot inhibiting strigolactones. The same trend was observed in root exudates of *max3* and *max4*, which showed low level of strigolactones in comparison to wild type (Umehara et al, 2008). A reduction in the levels of other carotenoid degradation products; i.e. apocarotenoids in the roots is also possible. For example, both *CCD7* and *CCD8* are also involved in β -

carotene catabolism (Booker et al., 2004; Auldridge et al., 2006), where they cleave the 9, 10 and 13, 14 double bonds of β -carotene to produce 10- β -carotenal and 13- β -carotenone, respectively (Ohmiya, 2009).

4.3 *MiR156* Exhibits Differential Effects on Expression of *CCD/NCED* Genes

In the siliques, the transcript levels of *CCD7*, *NCED2*, *NCED3*, *NCED5* and *NCED9* were significantly lower in *sk156* and *RS105* compared to the wild type; however, this trend was different from that in the roots where the transcript levels of *CCD4*, *CCD7*, *CCD8*, *NCED2*, *NCED6* and *NCED9* were affected in both *sk156* and *RS105*. All five members of NCED proteins are involved in ABA synthesis, and they are targeted to plastids (Tan et al., 2003). My results showed that expression of *NCED6* was reduced only in the roots, whereas in the siliques, it showed a higher transcript level compared to wild type. ABA biosynthesis in Arabidopsis seeds is mainly regulated by the action of *NCED6* and *NCED9*, and their transcript levels were higher in comparison to *NCED2*, *NCED3* and *NCED5* (Lefebvre et al., 2006). In addition, the *nced6-nced9* double mutant in Arabidopsis showed reduced ABA levels and a dormancy period (Lefebvre et al., 2006). Based on my results, there were no significant changes observed in terms of seed germination and dormancy in *sk156* and *RS105*. Perhaps a reduction in expression of *NCED9* in the siliques of *sk156* and *RS105* was not significant enough to cause dormancy as was observed in the *nced6-nced9* double mutant. In contrast to the roots, *CCD8* was unaffected in the siliques. Since *sk156* showed increased levels of β -carotene in seeds, probably *CCD7* has a stronger effect on β -carotene accumulation in this organ.

4.4 The Effect of *SPL15* on the Transcript Level of *CCD/NCED* Genes

As *SPL15* is active in the vegetative shoot apex; *SPL15* mutant phenotypes were found to affect vegetative development, including juvenile-to-adult phase transition (Schwarz et al., 2008). In addition, *SPL15* loss-of-function leads to enhanced branching, altered inflorescence architecture and shortened plastochron during vegetative growth (Schwarz et al., 2008). My results showed that the transcript levels of *CCD4*, *CCD7*, *NCED2* and *NCED9* in the roots, and *NCED3* and *NCED9*, in the siliques were significantly lower in 35S:*SPL15* (*SPL15* overexpression) lines relative to wild type, but *CCD8* and *NCED2* were unaffected in siliques and *NCED3* in roots. Therefore, the higher transcript level of *SPL15* in 35S:*SPL15* lines do not necessarily lead to higher transcript levels of *CCD/NCED* genes. Transgenic *sk156* plants overexpressing native *SPL15* had a *sk156* phenotype, whereas those overexpressing a mutated (*miR156* insensitive) *SPL15* (35S:*SPL15m*) showed a wild type phenotype and reduced *miR156* transcript levels (Wei et al., 2012). This led the authors to suggest and ultimately proved that *SPL15* had a negative regulatory effect on its cognate *miR156* regulator (Wei et al., 2012). My results showed that enhanced *SPL15* expression had a negative effect on the expression of some *CCD/NCED* genes including, *CCD7*, *NCED2*, and *NCED9*, and also up-regulated *CCD8*, *NCED5* and *NCED6* which suggests that *SPL15*, perhaps only when overexpressed, can have a silencing effect on at least some *CCD/NCED* genes. A negative regulatory effect of *miR156* and target genes on downstream genes is corroborated by earlier findings on the negative regulation of anthocyanin biosynthesis genes by *SPL9* in Arabidopsis (Gou et al., 2011). My results showed that in *spl15* the transcript levels of all *CCD/NCED* genes in roots were significantly decreased compared to wild type and also except for *CCD1* and *NCED6*, the transcript levels of other *CCD/NCED* genes in

siliques were significantly lower in comparison to wild type. These findings confirm my hypothesis that at least some *CCD/NCED* genes are positively regulated by *SPL15*.

The numbers and locations of the of GTAC core element vary among *CCD* and *NCED* promoters (Fig 7). *SPL15* exerts different effects on the transcript levels of different *CCD* and *NCED* genes in the roots and siliques. The results in both the roots and siliques revealed that *CCD4*, *CCD8*, *NCED5* and *NCED6* had significantly higher transcript levels compared to wild type; however, *CCD7*, *NCED2*, *NCED3* and *NCED9* were unaffected. Interestingly, the number of GTAC elements in the promoter regions of *CCD4*, *CCD8*, *NCED5* and *NCED6* were 3, 4, 2 and 3 respectively, which were less than those in the promoter regions of *CCD7*, *NCED2*, *NCED3* and *NCED9*, which contain 4, 5, 4 and 8 GTAC elements, respectively. Therefore, the number of GTAC elements in the promoter regions of *CCD* and *NCED* did not correlate with effects on the transcript levels of *CCD/NCED* genes, as only those with lower numbers of GTAC elements was affected by *SPL15*. Among the *CCD/NCED* genes affected by *SPL15*, GTAC elements were present between 500 and 1550 bp upstream of the translation start codon, and thus I conclude that this region, and not the number of GTAC elements, may be critical for *CCD/NCED* regulation by *SPL15*.

4.5 SPL15 Binding to Promoters of *CCD/NCED* Genes

The binding of SPL proteins to promoters of some genes in the miR156/SPL regulatory network has been previously demonstrated (Yamaguchi et al., 2009). My ChIP-qPCR analysis demonstrated that *SPL15* can bind to the promoters of *CCD4*, *CCD8*, *NCED5* and *NCED6*, even though there were variations in the binding capacity in different genes, and even to different GTAC elements within the same promoter. These results suggest a selective

binding of SPL15 to regions within the *CCD/NCED* promoters. In addition, the *in silico* analysis showed the importance of sequences immediately up-stream and down-stream of the GTAC core element for SPL15 binding efficiency.

4.6 Overexpression of miR156 Affects the Anatomical Structure of Plastids in Seeds

In oilseeds, including *Arabidopsis*, carotenoids can be stored in seed elaioplasts, where carotenoid production and storage is important for seed dormancy, ABA production and antioxidant systems (Calucci et al., 2004; Frey et al., 2012). Although the metabolic pathways that control carotenoid biosynthesis and catabolism are essentially known, and together play a significant role in determining the steady-state level of carotenoids, the capacity and size of plastids to store carotenoids has a direct bearing on carotenoid accumulation as well (Cazzonelli and Pogson, 2010). Even though all carotenoid biosynthesis genes are encoded by the nuclear genome, nearly all carotenoid pigments and their enzymes are located in the plastid (Cazzonelli et al., 2009).

Transmission electron micrographs of elaioplasts from mature *sk156*, *RS105* and wild type seeds showed plastoglobules as round particles on the thylakoid membranes of plastids (Fig 8), which is consistent with earlier studies (Austin et al., 2006; Brehelin et al., 2007; Nacir and Brehelin, 2013). The numbers of plastoglobules are dependent on plastid development and plastoglobules biogenesis (Kroll et al., 2001; Austin et al., 2006; Rudella et al., 2006). The number of plastoglobules that I detected by analyzing electron micrographs of elaioplasts of *sk156*, *RS105* and wild type seems to be higher than that found in chloroplasts by Brehelin and Kessler (2008). The same trend was observed in the etioplast, where the number of plastoglobules were reported to be more than in chloroplasts (Lichtenthaler and

Peveling, 1966). In some oilseed species, such as *Arabidopsis* and *Brassica napus*, elaioplasts are specialized to store lipids at high levels even to a higher range than amyloplasts (Shewmaker et al., 1999). My results showed that there is a link between enhanced carotenoid accumulation and the size of elaioplasts. Electron micrographs of *sk156* showed that the average size of a total of 35 elaioplasts is significantly larger compared to wild type. *RS105* also showed a larger plastid size compared to wild type, but not as large as that of *sk156*. This may be due to differences in levels of *miR156* expression; with *sk156* showing higher expression than *RS105*. This is also consistent with *sk156* mutant having a higher level of some carotenoids, such as lutein, β -carotene, violaxanthin and zeaxanthin (Wei et al., 2012). Thus, I conclude that enhanced carotenoid accumulation has a direct effect on elaioplasts size in *Arabidopsis* seeds, and that the ability of the cell to store and sequester carotenoids is a critical determinant of the steady-state level of carotenoids. Similar findings were reported in other plant species. For example, in *Brassica oleracea* (cauliflower) enhanced carotene accumulation in the *Or* mutant is accompanied by an increase in the size of chromoplasts (Paolillo et al., 2004). Also the *high pigment 2 (hp-2)* tomato mutant showed high levels of lycopene and larger plastids (Kolotilin et al., 2007). Similarly, the *high pigmentation 3 (hp-3)* mutant of tomato, which has a lesion in zeaxanthin epoxidase and deficiency in ABA, has a larger plastid compartment and 30% more storage capacity compared to wild type (Galpaz et al., 2008). Besides the size of elaioplasts, the plastoglobules in *sk156* and *RS105* showed a larger size compared to those in wild type. Based on my results, I conclude that there is a link between the level of carotenoid accumulation and the sizes of the elaioplasts and plastoglobules in *Arabidopsis* seeds.

4.7 Conclusions and Prospective for Future Research

In my research, the involvement of *miR156* and *SPL15* in carotenoid accumulation was assessed. I investigated the effect of *miR156* and *SPL15* on the transcript levels of *CCD/NCED* gene family by qRT-PCR, and determined the ability of *SPL15* to bind to the promoter regions of *CCD* and *NCED* genes using ChIP-qPCR. In addition, the effect of *miR156* on the anatomical structure of elaioplasts in the *Arabidopsis* seeds was investigated by using transmission electron microscopy. The results revealed that the expression of most of the *CCD/NCED* genes was affected by *miR156*, albeit the effects were different between siliques and roots. My results also suggest that higher transcript levels of *SPL15* do not necessarily lead activation of all *CCD/NCED* genes, as some of them were in fact silenced or not affected at all by *SPL15*. The ChIP-qPCR confirmed the strong and selective binding of *SPL15* to the promoter regions of *CCD/NCED* genes. These findings are in agreement with the hypothesis, that some of the *CCD/NCED* genes are affected by either *miR156* or *SPL15*, and further they have a regulatory effect on carotenoid accumulation in *Arabidopsis* seeds. The electron micrographs of elaioplasts in *Arabidopsis* seeds revealed the increased size of elaioplasts in the seeds of *sk156* and *RS105* compared to wild type. Moreover, the sizes of plastoglobules in elaioplasts of *sk156* and *RS105* were increased in comparison to wild type. This part of the results was in agreement with previous studies, which showed that increased levels of carotenoids in cauliflower and tomato was accompanied by enhanced size of plastids (Paolillo et al., 2004; Kolotilin et al., 2007). In conclusion, my result confirmed that the negative regulatory effect of *miR156* on the expression of some *CCD* and *NCED* genes. Also the strong *SPL15* occupancy on promoter regions of some *CCD/NCED* genes confirmed the regulatory effect of *SPL15* on these genes. Lastly, *miR156* caused enhanced carotenoid accumulation, and this was accompanied by increased sizes of plastids and

plastoglobules in the seeds. These findings are illustrated in a proposed model for miR156 and SPL15 role in regulating carotenoid accumulation (Fig. 14). SPL15 activates at least some of the *CCD/NCED* genes, and that suppression of *SPL15* by *miR156* leads to reduced *CCD/NCED* expression, reduced carotenoid catabolism, and hence enhanced carotenoid accumulation. These effects are also accompanied by an increase in the size of elaioplasts allowing for greater accumulation of seed carotenoids.

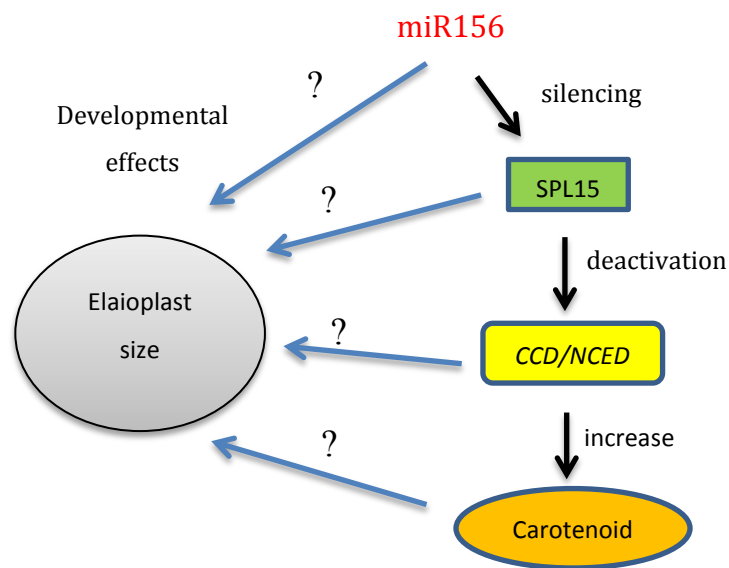


Figure 14. A proposed model for the regulatory role of miR156 in carotenoid accumulation

Future studies should include investigation of levels apocarotenoids, including strigolactones, in the mutants and lines that were used in this study to reveal the link between suppressed *CCD/NCED* genes and their specific products in Arabidopsis seeds. This information can be further used to improve the carotenoid profiles of economically important crops.

Of all SPLs, SPL9 showed high similarity to SPL15 at both the amino sequence and function, which was evident from the similar phenotypes of both, *spl15* and *spl9* knockout mutants (Schwarz et al., 2008). Both SPL9 and SPL15 also seem to function, at least partly, as suppressors of their target genes (Gou et al., 2011; our study). Therefore, further experiments to analyze the regulatory effects of *miR156* on other *SPL* genes, specifically *SPL9*, would be needed for a full understanding of the role of these genes in carotenoid catabolism.

The results of this study could have applications in improving the carotenoid profiles of plants, especially oilseed crops, such as canola, flax and soybean.

References

- Akiyama, K., Matsuzaki, K., and Hayashi, H.** (2005). Plant sesquiterpenes induce hyphal branching in arbuscular mycorrhizal fungi. *Nature* **435**, 824-827.
- Albrecht, V., Estavillo, G.M., Cuttriss, A.J., and Pogson, B.J.** (2011). Identifying chloroplast biogenesis and signalling mutants in *Arabidopsis thaliana*. *Methods Mol Biol* **684**, 257-272.
- Arazi, T., Talmor-Neiman, M., Stav, R., Riese, M., Huijser, P., and Baulcombe, D.C.** (2005). Cloning and characterization of micro-RNAs from moss. *Plant J* **43**, 837-848.
- Auldridge, M.E., Block, A., Vogel, J.T., Dabney-Smith, C., Mila, I., Bouzayen, M., Magallanes-Lundback, M., DellaPenna, D., McCarty, D.R., and Klee, H.J.** (2006). Characterization of three members of the *Arabidopsis* carotenoid cleavage dioxygenase family demonstrates the divergent roles of this multifunctional enzyme family. *Plant J* **45**, 982-993.
- Austin, J.R., 2nd, Frost, E., Vidi, P.A., Kessler, F., and Staehelin, L.A.** (2006). Plastoglobules are lipoprotein subcompartments of the chloroplast that are permanently coupled to thylakoid membranes and contain biosynthetic enzymes. *Plant Cell* **18**, 1693-1703.
- Balmer, Y., Vensel, W.H., DuPont, F.M., Buchanan, B.B., and Hurkman, W.J.** (2006). Proteome of amyloplasts isolated from developing wheat endosperm presents evidence of broad metabolic capability. *J Exp Bot* **57**, 1591-1602.
- Bartel, D.P.** (2004). MicroRNAs: genomics, biogenesis, mechanism, and function. *Cell* **116**, 281-297.
- Beisel, K.G., Jahnke, S., Hofmann, D., Koppchen, S., Schurr, U., and Matsubara, S.** (2010). Continuous turnover of carotenes and chlorophyll a in mature leaves of *Arabidopsis* revealed by ¹⁴CO₂ pulse-chase labeling. *Plant Physiol* **152**, 2188-2199.
- Ben-Amotz, A., and Fishler, R.** (1998). Analysis of carotenoids with emphasis on 9-cis beta-carotene in vegetables and fruits commonly consumed in Israel. *Food Chemistry* **62**, 515-520.
- Birkenbihl, R.P., Jach, G., Saedler, H., and Huijser, P.** (2005). Functional dissection of the plant-specific SBP-domain: overlap of the DNA-binding and nuclear localization domains. *J Mol Biol* **352**, 585-596.
- Booker, J., Auldridge, M., Wills, S., McCarty, D., Klee, H., and Leyser, O.** (2004). MAX3/CCD7 is a carotenoid cleavage dioxygenase required for the synthesis of a novel plant signaling molecule. *Curr Biol* **14**, 1232-1238.

- Bouvier, F., Isner, J.C., Dogbo, O., and Camara, B.** (2005). Oxidative tailoring of carotenoids: a prospect towards novel functions in plants. *Trends Plant Sci* **10**, 187-194.
- Brehelin, C., and Kessler, F.** (2008). The plastoglobule: a bag full of lipid biochemistry tricks. *Photochem Photobiol* **84**, 1388-1394.
- Brehelin, C., Kessler, F., and van Wijk, K.J.** (2007). Plastoglobules: versatile lipoprotein particles in plastids. *Trends Plant Sci* **12**, 260-266.
- Britton, G., Liaaen-Jensen, S., and Pfander, H.P.** (2004). *Carotenoids: Handbook*. (Springer Verlag).
- Brodersen, P., Sakvarelidze-Achard, L., Bruun-Rasmussen, M., Dunoyer, P., Yamamoto, Y.Y., Sieburth, L., and Voinnet, O.** (2008). Widespread translational inhibition by plant miRNAs and siRNAs. *Science* **320**, 1185-1190.
- Burbidge, A., Grieve, T.M., Jackson, A., Thompson, A., McCarty, D.R., and Taylor, I.B.** (1999). Characterization of the ABA-deficient tomato mutant *notabilis* and its relationship with maize Vp14. *Plant J* **17**, 427-431.
- Calucci, L., Capocchi, A., Galleschi, L., Ghiringhelli, S., Pinzino, C., Saviozzi, F., and Zandomenighi, M.** (2004). Antioxidants, free radicals, storage proteins, puuroindolines, and proteolytic activities in bread wheat (*Triticum aestivum*) seeds during accelerated aging. *J Agric Food Chem* **52**, 4274-4281.
- Cardon, G., Hohmann, S., Klein, J., Nettlesheim, K., Saedler, H., and Huijser, P.** (1999). Molecular characterisation of the Arabidopsis SBP-box genes. *Gene* **237**, 91-104.
- Cardon, G.H., Hohmann, S., Nettlesheim, K., Saedler, H., and Huijser, P.** (1997). Functional analysis of the Arabidopsis thaliana SBP-box gene SPL3: a novel gene involved in the floral transition. *Plant J* **12**, 367-377.
- Cazzonelli, C.I.** (2011). Carotenoids in nature: insights from plants and beyond. *Functional plant biology FPB*. **38**, 833-847.
- Cazzonelli, C.I., and Pogson, B.J.** (2010). Source to sink: regulation of carotenoid biosynthesis in plants. *Trends Plant Sci* **15**, 266-274.
- Cazzonelli, C.I., Cuttriss, A.J., Cossetto, S.B., Pye, W., Crisp, P., Whelan, J., Finnegan, E.J., Turnbull, C., and Pogson, B.J.** (2009). Regulation of carotenoid composition and shoot branching in Arabidopsis by a chromatin modifying histone methyltransferase, SDG8. *Plant Cell* **21**, 39-53.
- Chernys, J.T., and Zeevaart, J.A.** (2000). Characterization of the 9-cis-epoxycarotenoid dioxygenase gene family and the regulation of abscisic acid biosynthesis in avocado. *Plant Physiol* **124**, 343-353.

- Cook, C.E., Whichard, L.P., Turner, B., Wall, M.E., and Egley, G.H.** (1966). Germination of Witchweed (*Striga lutea* Lour.): Isolation and Properties of a Potent Stimulant. *Science* **154**, 1189-1190.
- Deruere, J., Romer, S., d'Harlingue, A., Backhaus, R.A., Kuntz, M., and Camara, B.** (1994). Fibril assembly and carotenoid overaccumulation in chromoplasts: a model for supramolecular lipoprotein structures. *Plant Cell* **6**, 119-133.
- Fraser, P.D., Enfissi, E.M., Halket, J.M., Truesdale, M.R., Yu, D., Gerrish, C., and Bramley, P.M.** (2007). Manipulation of phytoene levels in tomato fruit: effects on isoprenoids, plastids, and intermediary metabolism. *Plant Cell* **19**, 3194-3211.
- Fратиани, A., Irano, M., Panfili, G., and Acquistucci, R.** (2005). Estimation of color of durum wheat. Comparison of WSB, HPLC, and reflectance colorimeter measurements. *J Agric Food Chem* **53**, 2373-2378.
- Frey, A., Godin, B., Bonnet, M., Sotta, B., and Marion-Poll, A.** (2004). Maternal synthesis of abscisic acid controls seed development and yield in *Nicotiana plumbaginifolia*. *Planta* **218**, 958-964.
- Frey, A., Effroy, D., Lefebvre, V., Seo, M., Perreau, F., Berger, A., Sechet, J., To, A., North, H.M., and Marion-Poll, A.** (2012). Epoxycarotenoid cleavage by NCED5 fine-tunes ABA accumulation and affects seed dormancy and drought tolerance with other NCED family members. *Plant J* **70**, 501-512.
- Fu, C., Sunkar, R., Zhou, C., Shen, H., Zhang, J.Y., Matts, J., Wolf, J., Mann, D.G., Stewart, C.N., Jr., Tang, Y., and Wang, Z.Y.** (2012). Overexpression of miR156 in switchgrass (*Panicum virgatum* L.) results in various morphological alterations and leads to improved biomass production. *Plant Biotechnol J* **10**, 443-452.
- Galpaz, N., Wang, Q., Menda, N., Zamir, D., and Hirschberg, J.** (2008). Abscisic acid deficiency in the tomato mutant high-pigment 3 leading to increased plastid number and higher fruit lycopene content. *Plant J* **53**, 717-730.
- Gandikota, M., Birkenbihl, R.P., Hohmann, S., Cardon, G.H., Saedler, H., and Huijser, P.** (2007). The miRNA156/157 recognition element in the 3' UTR of the Arabidopsis SBP box gene *SPL3* prevents early flowering by translational inhibition in seedlings. *Plant J* **49**, 683-693.
- Garcia-Limones, C., Schnabele, K., Blanco-Portales, R., Luz Bellido, M., Caballero, J.L., Schwab, W., and Munoz-Blanco, J.** (2008). Functional characterization of FaCCD1: a carotenoid cleavage dioxygenase from strawberry involved in lutein degradation during fruit ripening. *J Agric Food Chem* **56**, 9277-9285.
- Ghosh, S., Hudak, K.A., Dumbroff, E.B., and Thompson, J.E.** (1994). Release of Photosynthetic Protein Catabolites by Blebbing from Thylakoids. *Plant Physiol* **106**, 1547-1553.

- Giovannoni, J.** (2001). Molecular Biology of Fruit Maturation and Ripening. *Annu Rev Plant Physiol Plant Mol Biol* **52**, 725-749.
- Gomez-Roldan, V., Fermas, S., Brewer, P.B., Puech-Pages, V., Dun, E.A., Pilot, J.P., Letisse, F., Matusova, R., Danoun, S., Portais, J.C., Bouwmeester, H., Becard, G., Beveridge, C.A., Rameau, C., and Rochange, S.F.** (2008). Strigolactone inhibition of shoot branching. *Nature* **455**, 189-194.
- Gou, J.Y., Felippes, F.F., Liu, C.J., Weigel, D., and Wang, J.W.** (2011). Negative regulation of anthocyanin biosynthesis in Arabidopsis by a miR156-targeted SPL transcription factor. *Plant Cell* **23**, 1512-1522.
- Guo, A.Y., Zhu, Q.H., Gu, X., Ge, S., Yang, J., and Luo, J.** (2008). Genome-wide identification and evolutionary analysis of the plant specific SBP-box transcription factor family. *Gene* **418**, 1-8.
- Hashimoto, H., and Possingham, J.V.** (1989). Effect of light on the chloroplast division cycle and DNA synthesis in cultured leaf discs of spinach. *Plant Physiol* **89**, 1178-1183.
- Havaux, M., Dall'osto, L., and Bassi, R.** (2007). Zeaxanthin has enhanced antioxidant capacity with respect to all other xanthophylls in Arabidopsis leaves and functions independent of binding to PSII antennae. *Plant Physiol* **145**, 1506-1520.
- Howitt, C.A., and Pogson, B.J.** (2006). Carotenoid accumulation and function in seeds and non-green tissues. *Plant Cell Environ* **29**, 435-445.
- Huang, F.C., Horvath, G., Molnar, P., Turcsi, E., Deli, J., Schrader, J., Sandmann, G., Schmidt, H., and Schwab, W.** (2009). Substrate promiscuity of RdCCD1, a carotenoid cleavage oxygenase from *Rosa damascena*. *Phytochemistry* **70**, 457-464.
- Ilg, A., Beyer, P., and Al-Babili, S.** (2009). Characterization of the rice carotenoid cleavage dioxygenase 1 reveals a novel route for geranyl biosynthesis. *Febs J* **276**, 736-747.
- Iniesta, A.A., Cervantes, M., and Murillo, F.J.** (2008). Conversion of the lycopene monocyclase of *Myxococcus xanthus* into a bicyclase. *Appl Microbiol Biotechnol* **79**, 793-802.
- Irigoyen, S., Karlsson, P.M., Kuruvilla, J., Spetea, C., and Versaw, W.K.** (2011). The sink-specific plastidic phosphate transporter PHT4;2 influences starch accumulation and leaf size in Arabidopsis. *Plant Physiol* **157**, 1765-1777.
- Ishikawa, S., Maekawa, M., Arite, T., Onishi, K., Takamura, I., and Kyojuka, J.** (2005). Suppression of tiller bud activity in tillering dwarf mutants of rice. *Plant Cell Physiol* **46**, 79-86.
- Kanno, Y., Jikumaru, Y., Hanada, A., Nambara, E., Abrams, S.R., Kamiya, Y., and Seo, M.** (2010). Comprehensive hormone profiling in developing Arabidopsis seeds:

examination of the site of ABA biosynthesis, ABA transport and hormone interactions. *Plant Cell Physiol* **51**, 1988-2001.

- Kaup, M.T., Froese, C.D., and Thompson, J.E.** (2002). A role for diacylglycerol acyltransferase during leaf senescence. *Plant Physiol* **129**, 1616-1626.
- Kessler, F., Schnell, D., and Blobel, G.** (1999). Identification of proteins associated with plastoglobules isolated from pea (*Pisum sativum* L.) chloroplasts. *Planta* **208**, 107-113.
- Klee, H.J., and Giovannoni, J.J.** (2011). Genetics and control of tomato fruit ripening and quality attributes. *Annu Rev Genet* **45**, 41-59.
- Klein, J., Saedler, H., and Huijser, P.** (1996). A new family of DNA binding proteins includes putative transcriptional regulators of the *Antirrhinum majus* floral meristem identity gene SQUAMOSA. *Mol Gen Genet* **250**, 7-16.
- Kohler, R.H., and Hanson, M.R.** (2000). Plastid tubules of higher plants are tissue-specific and developmentally regulated. *J Cell Sci* **113** (Pt 1), 81-89.
- Kolotilin, I., Koltai, H., Tadmor, Y., Bar-Or, C., Reuveni, M., Meir, A., Nahon, S., Shlomo, H., Chen, L., and Levin, I.** (2007). Transcriptional profiling of high pigment-2dg tomato mutant links early fruit plastid biogenesis with its overproduction of phytonutrients. *Plant Physiol* **145**, 389-401.
- Kroll, D., Meierhoff, K., Bechtold, N., Kinoshita, M., Westphal, S., Vothknecht, U.C., Soll, J., and Westhoff, P.** (2001). VIPP1, a nuclear gene of *Arabidopsis thaliana* essential for thylakoid membrane formation. *Proc Natl Acad Sci U S A* **98**, 4238-4242.
- Kropat, J., Tottey, S., Birkenbihl, R.P., Depege, N., Huijser, P., and Merchant, S.** (2005). A regulator of nutritional copper signaling in *Chlamydomonas* is an SBP domain protein that recognizes the GTAC core of copper response element. *Proc Natl Acad Sci U S A* **102**, 18730-18735.
- Lannenpaa, M., Janonen, I., Holttä-Vuori, M., Gardemeister, M., Porali, I., and Sopanen, T.** (2004). A new SBP-box gene BpSPL1 in silver birch (*Betula pendula*). *Physiologia Plantarum* **120**, 491-500.
- Lefebvre, V., North, H., Frey, A., Sotta, B., Seo, M., Okamoto, M., Nambara, E., and Marion-Poll, A.** (2006). Functional analysis of *Arabidopsis* NCED6 and NCED9 genes indicates that ABA synthesized in the endosperm is involved in the induction of seed dormancy. *Plant J* **45**, 309-319.
- Li, F., Vallabhaneni, R., Yu, J., Rocheford, T., and Wurtzel, E.T.** (2008). The maize phytoene synthase gene family: overlapping roles for carotenogenesis in endosperm, photomorphogenesis, and thermal stress tolerance. *Plant Physiol* **147**, 1334-1346.

- Liang, X., Nazareus, T.J., and Stone, J.M.** (2008). Identification of a consensus DNA-binding site for the *Arabidopsis thaliana* SBP domain transcription factor, AtSPL14, and binding kinetics by surface plasmon resonance. *Biochemistry* **47**, 3645-3653.
- Lichtenthaler, H.K., and Peveling, E.** (1966). [Osmiophilic lipid inclusions in the chloroplasts and in the cytoplasm of *Hoya carnosa* R. Br]. *Naturwissenschaften* **53**, 534.
- Lindgren, L.O., Stalberg, K.G., and Hoglund, A.S.** (2003). Seed-specific overexpression of an endogenous *Arabidopsis* phytoene synthase gene results in delayed germination and increased levels of carotenoids, chlorophyll, and abscisic acid. *Plant Physiol* **132**, 779-785.
- Lindqvist, A., and Andersson, S.** (2002). Biochemical properties of purified recombinant human beta-carotene 15,15'-monooxygenase. *J Biol Chem* **277**, 23942-23948.
- Llave, C., Kasschau, K.D., Rector, M.A., and Carrington, J.C.** (2002). Endogenous and silencing-associated small RNAs in plants. *Plant Cell* **14**, 1605-1619.
- Lopez-Raez, J.A., Charnikhova, T., Gomez-Roldan, V., Matusova, R., Kohlen, W., De Vos, R., Verstappen, F., Puech-Pages, V., Becard, G., Mulder, P., and Bouwmeester, H.** (2008). Tomato strigolactones are derived from carotenoids and their biosynthesis is promoted by phosphate starvation. *New Phytol* **178**, 863-874.
- Matus, Z., Molnar, P., and Szabo, L.G.** (1993). [Main carotenoids in pressed seeds (*Cucurbitae semen*) of oil pumpkin (*Cucurbita pepo convar. pepo var. styriaca*)]. *Acta Pharm Hung* **63**, 247-256.
- Matusova, R., Rani, K., Verstappen, F.W., Franssen, M.C., Beale, M.H., and Bouwmeester, H.J.** (2005). The strigolactone germination stimulants of the plant-parasitic *Striga* and *Orobanche* spp. are derived from the carotenoid pathway. *Plant Physiol* **139**, 920-934.
- McGraw, K.J., Hill, G.E., Stradi, R., and Parker, R.S.** (2001). The influence of carotenoid acquisition and utilization on the maintenance of species-typical plumage pigmentation in male American goldfinches (*Carduelis tristis*) and northern cardinals (*Cardinalis cardinalis*). *Physiol Biochem Zool* **74**, 843-852.
- Meier, S., Tzfadia, O., Vallabhaneni, R., Gehring, C., and Wurtzel, E.T.** (2011). A transcriptional analysis of carotenoid, chlorophyll and plastidial isoprenoid biosynthesis genes during development and osmotic stress responses in *Arabidopsis thaliana*. *BMC Syst Biol* **5**, 77.
- Moehs, C.P., Tian, L., Osteryoung, K.W., and Dellapenna, D.** (2001). Analysis of carotenoid biosynthetic gene expression during marigold petal development. *Plant Mol Biol* **45**, 281-293.
- Moran, N.A., and Jarvik, T.** (2010). Lateral transfer of genes from fungi underlies carotenoid production in aphids. *Science* **328**, 624-627.

- Nacir, H., and Brehelin, C.** (2013). When proteomics reveals unsuspected roles: the plastoglobule example. *Front Plant Sci* **4**, 114.
- Nambara, E., and Marion-Poll, A.** (2005). Abscisic acid biosynthesis and catabolism. *Annu Rev Plant Biol* **56**, 165-185.
- Navarro, L., Dunoyer, P., Jay, F., Arnold, B., Dharmasiri, N., Estelle, M., Voinnet, O., and Jones, J.D.** (2006). A plant miRNA contributes to antibacterial resistance by repressing auxin signaling. *Science* **312**, 436-439.
- Neuhaus, H.E., and Emes, M.J.** (2000). Nonphotosynthetic metabolism in plastids. In *Annual Review of Plant Physiology and Plant Molecular Biology; Annual Review of Plant Physiology and Plant Molecular Biology*, 4139 El Camino Way, Palo Alto, CA, 94303-0139, USA), pp. 111-140.
- Ohmiya, A.** (2009). Carotenoid cleavage dioxygenases and their apocarotenoid products in plants. *Plant Biotechnology* **26**, 351-358.
- Ohmiya, A., Kishimoto, S., Aida, R., Yoshioka, S., and Sumitomo, K.** (2006). Carotenoid cleavage dioxygenase (CmCCD4a) contributes to white color formation in chrysanthemum petals. *Plant Physiol* **142**, 1193-1201.
- Paolillo, D.J., Jr., Garvin, D.F., and Parthasarathy, M.V.** (2004). The chromoplasts of Or mutants of cauliflower (*Brassica oleracea* L. var. botrytis). *Protoplasma* **224**, 245-253.
- Polivka, T., and Frank, H.A.** (2010). Molecular factors controlling photosynthetic light harvesting by carotenoids. *Acc Chem Res* **43**, 1125-1134.
- Pozueta-Romero, J., Rafia, F., Houlne, G., Cheniclet, C., Carde, J.P., Schantz, M.L., and Schantz, R.** (1997). A ubiquitous plant housekeeping gene, PAP, encodes a major protein component of bell pepper chromoplasts. *Plant Physiol* **115**, 1185-1194.
- Redmond, T.M., Gentleman, S., Duncan, T., Yu, S., Wiggert, B., Gantt, E., and Cunningham, F.X., Jr.** (2001). Identification, expression, and substrate specificity of a mammalian beta-carotene 15,15'-dioxygenase. *J Biol Chem* **276**, 6560-6565.
- Rhoades, M.W., Reinhart, B.J., Lim, L.P., Burge, C.B., Bartel, B., and Bartel, D.P.** (2002). Prediction of plant microRNA targets. *Cell* **110**, 513-520.
- Rubio, A., Rambla, J.L., Santaella, M., Gomez, M.D., Orzaez, D., Granell, A., and Gomez-Gomez, L.** (2008). Cytosolic and plastoglobule-targeted carotenoid dioxygenases from *Crocus sativus* are both involved in beta-ionone release. *J Biol Chem* **283**, 24816-24825.
- Rudella, A., Friso, G., Alonso, J.M., Ecker, J.R., and van Wijk, K.J.** (2006). Downregulation of ClpR2 leads to reduced accumulation of the ClpPRS protease complex and defects in chloroplast biogenesis in *Arabidopsis*. *Plant Cell* **18**, 1704-1721.

- Ruiz-Sola, M.A., and Rodriguez-Concepcion, M.** (2012). Carotenoid biosynthesis in Arabidopsis: a colorful pathway. *Arabidopsis Book* **10**, e0158.
- Sandmann, G., Romer, S., and Fraser, P.D.** (2006). Understanding carotenoid metabolism as a necessity for genetic engineering of crop plants. *Metab Eng* **8**, 291-302.
- Schmidt, H., Kurtzer, R., Eisenreich, W., and Schwab, W.** (2006). The carotenase AtCCD1 from Arabidopsis thaliana is a dioxygenase. *J Biol Chem* **281**, 9845-9851.
- Schwab, R., Palatnik, J.F., Riester, M., Schommer, C., Schmid, M., and Weigel, D.** (2005). Specific effects of microRNAs on the plant transcriptome. *Dev Cell* **8**, 517-527.
- Schwarz, S., Grande, A.V., Bujdoso, N., Saedler, H., and Huijser, P.** (2008). The microRNA regulated SBP-box genes SPL9 and SPL15 control shoot maturation in Arabidopsis. *Plant Mol Biol* **67**, 183-195.
- Shewmaker, C.K., Sheehy, J.A., Daley, M., Colburn, S., and Ke, D.Y.** (1999). Seed-specific overexpression of phytoene synthase: increase in carotenoids and other metabolic effects. *Plant J* **20**, 401-412X.
- Simkin, A.J., Underwood, B.A., Auldridge, M., Loucas, H.M., Shibuya, K., Schmelz, E., Clark, D.G., and Klee, H.J.** (2004). Circadian regulation of the PhCCD1 carotenoid cleavage dioxygenase controls emission of beta-ionone, a fragrance volatile of petunia flowers. *Plant Physiol* **136**, 3504-3514.
- Sorefan, K., Booker, J., Haurogne, K., Goussot, M., Bainbridge, K., Foo, E., Chatfield, S., Ward, S., Beveridge, C., Rameau, C., and Leyser, O.** (2003). MAX4 and RMS1 are orthologous dioxygenase-like genes that regulate shoot branching in Arabidopsis and pea. *Genes Dev* **17**, 1469-1474.
- Stirnberg, P., van De Sande, K., and Leyser, H.M.** (2002). MAX1 and MAX2 control shoot lateral branching in Arabidopsis. *Development* **129**, 1131-1141.
- Tan, B.C., Joseph, L.M., Deng, W.T., Liu, L., Li, Q.B., Cline, K., and McCarty, D.R.** (2003). Molecular characterization of the Arabidopsis 9-cis epoxycarotenoid dioxygenase gene family. *Plant J* **35**, 44-56.
- Toledo-Ortiz, G., Huq, E., and Rodriguez-Concepcion, M.** (2010). Direct regulation of phytoene synthase gene expression and carotenoid biosynthesis by phytochrome-interacting factors. *Proc Natl Acad Sci U S A* **107**, 11626-11631.
- Umeno, D., Tobias, A.V., and Arnold, F.H.** (2005). Diversifying carotenoid biosynthetic pathways by directed evolution. *Microbiol Mol Biol Rev* **69**, 51-78.
- Usami, T., Horiguchi, G., Yano, S., and Tsukaya, H.** (2009). The more and smaller cells mutants of Arabidopsis thaliana identify novel roles for SQUAMOSA PROMOTER BINDING PROTEIN-LIKE genes in the control of heteroblasty. *Development* **136**, 955-964.

- Vishnevetsky, M., Ovadis, M., Zuker, A., and Vainstein, A.** (1999). Molecular mechanisms underlying carotenogenesis in the chromoplast: multilevel regulation of carotenoid-associated genes. *Plant J* **20**, 423-431.
- Walter, M.H., Floss, D.S., and Strack, D.** (2010). Apocarotenoids: hormones, mycorrhizal metabolites and aroma volatiles. *Planta* **232**, 1-17.
- Wang, Z., and Burge, C.B.** (2008). Splicing regulation: from a parts list of regulatory elements to an integrated splicing code. *RNA* **14**, 802-813.
- Wei, S., Yu, B., Gruber, M.Y., Khachatourians, G.G., Hegedus, D.D., and Hannoufa, A.** (2010). Enhanced seed carotenoid levels and branching in transgenic *Brassica napus* expressing the *Arabidopsis* miR156b gene. *J Agric Food Chem* **58**, 9572-9578.
- Wei, S., Gruber, M.Y., Yu, B., Gao, M.J., Khachatourians, G.G., Hegedus, D.D., Parkin, I.A., and Hannoufa, A.** (2012). *Arabidopsis* mutant sk156 reveals complex regulation of SPL15 in a miR156-controlled gene network. *BMC Plant Biol* **12**, 169.
- Welsch, R., Maass, D., Voegel, T., Dellapenna, D., and Beyer, P.** (2007). Transcription factor RAP2.2 and its interacting partner SINAT2: stable elements in the carotenogenesis of *Arabidopsis* leaves. *Plant Physiol* **145**, 1073-1085.
- Winter, D., Vinegar, B., Nahal, H., Ammar, R., Wilson, G.V., and Provart, N.J.** (2007). An "Electronic Fluorescent Pictograph" browser for exploring and analyzing large-scale biological data sets. *PLoS One* **2**, e718.
- Wu, G., Park, M.Y., Conway, S.R., Wang, J.W., Weigel, D., and Poethig, R.S.** (2009). The sequential action of miR156 and miR172 regulates developmental timing in *Arabidopsis*. *Cell* **138**, 750-759.
- Wurtzel, E.T., Cuttriss, A., and Vallabhaneni, R.** (2012). Maize provitamin a carotenoids, current resources, and future metabolic engineering challenges. *Front Plant Sci* **3**, 29.
- Xie, K., Shen, J., Hou, X., Yao, J., Li, X., Xiao, J., and Xiong, L.** (2012). Gradual increase of miR156 regulates temporal expression changes of numerous genes during leaf development in rice. *Plant Physiol* **158**, 1382-1394.
- Xie, X., and Yoneyama, K.** (2010). The strigolactone story. *Annu Rev Phytopathol* **48**, 93-117.
- Xie, X., Yoneyama, K., Kusumoto, D., Yamada, Y., Yokota, T., Takeuchi, Y., and Yoneyama, K.** (2008). Isolation and identification of alectrol as (+)-orobanchyl acetate, a germination stimulant for root parasitic plants. *Phytochemistry (Amsterdam)* **69**, 427-431.
- Yamaguchi, A., Wu, M.F., Yang, L., Wu, G., Poethig, R.S., and Wagner, D.** (2009). The microRNA-regulated SBP-Box transcription factor SPL3 is a direct upstream activator of LEAFY, FRUITFULL, and APETALA1. *Dev Cell* **17**, 268-278.

- Ytterberg, A.J., Peltier, J.B., and van Wijk, K.J.** (2006). Protein profiling of plastoglobules in chloroplasts and chromoplasts. A surprising site for differential accumulation of metabolic enzymes. *Plant Physiol* **140**, 984-997.
- Zhou, K., Su, L., and Yu, L.L.** (2004). Phytochemicals and antioxidant properties in wheat bran. *J Agric Food Chem* **52**, 6108-6114.

Appendix 1

Appendix 1. The BLAST search results of *CCD*, *NCED* and *SPL15* PCR products to determine their specificity

Arabidopsis thaliana chromosome 3, complete sequence

Sequence ID: [ref|NC_003074.8|](#) Length: 23459830 Number of Matches: 1

Range 1: 23455515 to 23455584 [GenBank](#) [Graphics](#) ▼ Next Match ▲ Previous Match

Score	Expect	Identities	Gaps	Strand
130 bits(70)	3e-30	70/70(100%)	0/70(0%)	Plus/Plus

Features: [carotenoid 9,10\(9',10'\)-cleavage dioxygenase 1](#)

```

Query 1          TGTTCGCGTGAGACAGCAGAAGAAGACGACGGTTACTTGATATTCITTTGTTTCATGATGA 60
                |||
Sbjct 23455515  TGTTCGCGTGAGACAGCAGAAGAAGACGACGGTTACTTGATATTCITTTGTTTCATGATGA 23455574

Query 61        AAACACAGGG 70
                |||
Sbjct 23455575  AAACACAGGG 23455584
  
```

Arabidopsis thaliana chromosome 4, complete sequence

Sequence ID: [ref|NC_003075.7|](#) Length: 18585056 Number of Matches: 1

Range 1: 10483317 to 10483371 [GenBank](#) [Graphics](#) ▼ Next Match ▲ Previous Match

Score	Expect	Identities	Gaps	Strand
102 bits(55)	5e-22	55/55(100%)	0/55(0%)	Plus/Minus

Features: [nine-cis-epoxycarotenoid dioxygenase 4](#)

```

Query 1          TTCTACGGGCCACCGTACAATCATCCCGATCTCCTTTAGACACATCAAGCTTCAC 55
                |||
Sbjct 10483371  TTCTACGGGCCACCGTACAATCATCCCGATCTCCTTTAGACACATCAAGCTTCAC 10483317
  
```

Arabidopsis thaliana chromosome 2, complete sequence

Sequence ID: [ref|NC_003071.7|](#) Length: 19698289 Number of Matches: 1

Range 1: 18560774 to 18560829 [GenBank](#) [Graphics](#) ▼ Next Match ▲ Previous Match

Score	Expect	Identities	Gaps	Strand
104 bits(56)	1e-22	56/56(100%)	0/56(0%)	Plus/Plus

Features: [carotenoid cleavage dioxygenase 7](#)

```

Query 1          GACTTTGGACTCTACCGGAAACTGCAATAGTTGTGATGTAGAGCCTCTAAACGGGT 56
                |||
Sbjct 18560774  GACTTTGGACTCTACCGGAAACTGCAATAGTTGTGATGTAGAGCCTCTAAACGGGT 18560829
  
```

Arabidopsis thaliana chromosome 4, complete sequence

Sequence ID: [ref|NC_003075.7|](#) Length: 18585056 Number of Matches: 1

Range 1: 15830984 to 15831059 [GenBank](#) [Graphics](#) ▼ Next Match ▲ Previous Match

Score	Expect	Identities	Gaps	Strand
141 bits(76)	2e-33	76/76(100%)	0/76(0%)	Plus/Plus

Features: [carotenoid cleavage dioxygenase 8](#)

```

Query 1          ATATTGTGGAGAAGAAAGTGAAGAAGTGGCAGCAGCATGGTATGATACCATCTGAACCAT 60
                |||
Sbjct 15830984  ATATTGTGGAGAAGAAAGTGAAGAAGTGGCAGCAGCATGGTATGATACCATCTGAACCAT 15831043

Query 61        TCTTCGTGCCITCGACC 76
                |||
Sbjct 15831044  TCTTCGTGCCITCGACC 15831059
  
```


Arabidopsis thaliana chromosome 4, complete sequence

Sequence ID: [ref|NC_003075.7|](#) Length: 18585056 Number of Matches: 410

Range 1: 10143203 to 10143241 [GenBank](#) [Graphics](#) ▼ Next Match ▲ Previous Match

Score	Expect	Identities	Gaps	Strand
77.8 bits(39)	1e-14	39/39(100%)	0/39(0%)	Plus/Plus

Features: [9-cis-epoxycarotenoid dioxygenase NCED2](#)

```

Query 1      AAAACCGAGAGATTGGTTCAGGAAAAACGATTGGGTCGA 39
            |||
Sbjct 10143203 AAAACCGAGAGATTGGTTCAGGAAAAACGATTGGGTCGA 10143241
  
```

Arabidopsis thaliana chromosome 3, complete sequence

Sequence ID: [ref|NC_003074.8|](#) Length: 23459830 Number of Matches: 1

Range 1: 4832993 to 4833045 [GenBank](#) [Graphics](#) ▼ Next Match ▲ Previous Match

Score	Expect	Identities	Gaps	Strand
99.0 bits(53)	3e-20	53/53(100%)	0/53(0%)	Plus/Plus

Features: [9-cis-epoxycarotenoid dioxygenase NCED3](#)

```

Query 117    TGAAGTGGGTTAGCTCCGTTGCGCACATACACTCCTTTGATGGAATCGGGAAG 169
            |||
Sbjct 4832993 TGAAGTGGGTTAGCTCCGTTGCGCACATACACTCCTTTGATGGAATCGGGAAG 4833045
  
```

Arabidopsis thaliana chromosome 1, complete sequence

Sequence ID: [ref|NC_003070.9|](#) Length: 30427671 Number of Matches: 1

Range 1: 10573031 to 10573088 [GenBank](#) [Graphics](#) ▼ Next Match ▲ Previous Match

Score	Expect	Identities	Gaps	Strand
108 bits(58)	1e-23	58/58(100%)	0/58(0%)	Plus/Plus

Features: [9-cis-epoxycarotenoid dioxygenase](#)

```

Query 1      AGCTTCATATTGTTAACGCCGTTACGTTGGAAGTAGAAGCAACCGTTAAATTGCCGTC 58
            |||
Sbjct 10573031 AGCTTCATATTGTTAACGCCGTTACGTTGGAAGTAGAAGCAACCGTTAAATTGCCGTC 10573088
  
```

Arabidopsis thaliana chromosome 3, complete sequence

Sequence ID: [ref|NC_003074.8|](#) Length: 23459830 Number of Matches: 1

Range 1: 8762078 to 8762136 [GenBank](#) [Graphics](#) ▼ Next Match ▲ Previous Match

Score	Expect	Identities	Gaps	Strand
110 bits(59)	3e-24	59/59(100%)	0/59(0%)	Plus/Plus

Features: [9-cis-epoxycarotenoid dioxygenase NCED6](#)

```

Query 1      ATCGGICTAGTGGACGGGACACGTGGCATGGGCGTAGCTAACGCCGGTGTGGTTTTCTT 59
            |||
Sbjct 8762078 ATCGGICTAGTGGACGGGACACGTGGCATGGGCGTAGCTAACGCCGGTGTGGTTTTCTT 8762136
  
```

Arabidopsis thaliana chromosome 3, complete sequence

Sequence ID: [ref|NC_003074.8|](#) Length: 23459830 Number of Matches: 1

Range 1: 21444630 to 21444711 [GenBank](#) [Graphics](#) ▼ Next Match ▲ Previous Match

Score	Expect	Identities	Gaps	Strand
152 bits(82)	8e-37	82/82(100%)	0/82(0%)	Plus/Minus

Features: [squamosa promoter-binding-like protein 15](#)

```

Query 1      TTCAACCCATCAGCCGCCATCTCAACACATCAGCAGTACCTCAGCCAAACTTGGGAAGT 60
            |||
Sbjct 21444711 TTCAACCCATCAGCCGCCATCTCAACACATCAGCAGTACCTCAGCCAAACTTGGGAAGT 21444652

Query 61      CATCGCGGGCGAAAAGAGCAAT 82
            |||
Sbjct 21444651 CATCGCGGGCGAAAAGAGCAAT 21444630
  
```

Curriculum Vitae

Name: Davood Emami Meybodi

Post-secondary Education and Degrees: M.Sc. Molecular Biology, 2011-2013
the University of Western Ontario
London, Ontario, Canada

M.Sc. Agricultural Biotechnology, 2003-2006
Mazandaran University
Sari, Mazandaran, Iran

B.Sc. Agricultural Engineering, 1998-2002
Islamic Azad University, Roudehen Branch

Honours and Awards Western Graduate Research Scholarship
2011 – 2013

Related Work Experience Teaching Assistant
the University of Western Ontario
2011-2013

Publications:

Emami Meybodi D, Torkamaned D, Danaee M, Hashemi M. 2011. The correlation of genetic diversity and geographic distribution of *Fusarium graminearum* in North part of Iran. *Pak J Biol Sci.* Vol 14: 831-837

Emami Meybodi D, Mozafari J, Babaeian N, Rahimian h. 2011. Application of electrotherapy for elimination of potato potyviruses. *J.Agr.Sci.Tech*, Vol 13:921-927.

Emami Meybodi, D., Mozafari, J., Babaeian N. and Rahimian H. 2008. Efficiency of serological techniques for detecting single and multiple infections of major potato viruses in the seed production system. *Iranian Journal of Plant Pathology*. Vol.43 (3):338-346

Book

Enayati Shariatpanahi, E. Shakib, M.A., and **Emami Meybodi, D.** 2011. Haploidy and its Applications in Modern Plant Breeding.